IEEE Access
Multidisciplinary | Rapid Review | Open Access Journal

Received June 8, 2021, accepted July 20, 2021, date of publication August 13, 2021, date of current version August 20, 2021.

Digital Object Identifier 10.1109/ACCESS.2021.3104464

Systematic Review of Intelligent Algorithms in Gait Analysis and Prediction for Lower Limb Robotic Systems

RANIA KOLAGHASSI, MOHAMAD KENAN AL-HARES, AND KONSTANTINOS SIRLANTZIS
Intelligent Interactions Research Group, University of Kent, Canterbury CT2 7NT, U.K.

Corresponding author: Rania Kolaghassi (rbk9@kent.ac.uk)

This work was supported by the Interreg 2 Seas Program 2014–2020 by the European Regional Development Fund (M.O.T.I.O.N Project) under Contract 2S05-038. The work of Rania Kolaghassi was supported by the Studentship through M.O.T.I.O.N. The work of Mohamad Kenan Al-Hares was supported by the M.O.T.I.O.N. Data through Kent Academic Repository (https://kar.kent.ac.uk/).

ABSTRACT The rate of development of robotic technologies has been meteoric, as a result of compounded advancements in hardware and software. Amongst these robotic technologies are active exoskeletons and orthoses, used in the assistive and rehabilitative fields. Artificial intelligence techniques are increasingly being utilised in gait analysis and prediction. This review paper systematically explores the current use of intelligent algorithms in gait analysis for robotic control, specifically the control of active lower limb exoskeletons and orthoses. Two databases, IEEE and Scopus, were screened for papers published between 1989 to May 2020. 41 papers met the eligibility criteria and were included in this review. 66.7% of the identified studies used classification models for the classification of gait phases and locomotion modes. Meanwhile, 33.3% implemented regression models for the estimation/prediction of kinematic parameters such as joint angles and trajectories, and kinetic parameters such as moments and torques. Deep learning algorithms have been deployed in ∼15% of the machine learning implementations. Other methodological parameters were reviewed, such as the sensor selection and the sample sizes used for training the models.

INDEX TERMS Gait analysis, exoskeletons, orthoses, machine learning, deep learning, wearable robotics, gait phases, locomotion, moments, joint angles.

I. INTRODUCTION

A plethora of wearable robotics devices that interface with humans, for varying medical and functional purposes, are being developed including exoskeletons and orthoses. An exoskeleton is an electro-mechanical device comprised of actuators, sensors, and controllers that provides torque to joints [1]. The provision of the supportive torque allows for physical actions to be performed with more ease and lower strain. Dating back to the 1960s, exoskeletons have been initially designed and developed for military use [1]. General Electric Company, developed Hardiman I exoskeleton, to augment the endurance and strength of the soldiers, leading to what was described as the 'union of man and machine' [2]. Half a century later, exoskeletons evolved to serve more purposes including industrial applications [3], rehabilitation, and restoration of gait for patients with Spinal Cord Injuries [4], Cerebral Palsy [5], and Multiple Sclerosis [6] to name a few. These exoskeletons are designed to support the upper limbs, lower limbs or the full-body and can be passive, active or quasi-passive [7]. Amongst the existing state of the art industrial exoskeletons is BLEEX, Berkeley Lower Extremity Exoskeleton, which is a seven degree of freedom exoskeleton. Actuated with linear hydraulics, it enables heavy load lifting in industrial settings [8]. The MIT exoskeleton is another quasi-passive exoskeleton for heavy load lifting, comprised of springs and dampers instead of actuators. It acts as an intermediator, transferring 80% of the load from the person to the ground [9]. HAL-5, Hybrid Assistive Limb, by the University of Tsukuba, is a full-body exoskeleton targeted for healthy people as well as patients and can enable paraplegics to walk by decoding their intentions [10]. MINDWALKER uses brain generated electroencephalogram (EEG) and electromyogram (EMG) signals to control a series of elastic actuated full-body exoskeleton targeted for paraplegics [11].

The associate editor coordinating the review of this manuscript and approving it for publication was Davide Patti.

Orthoses are another category of assistive and corrective technologies, sometimes used interchangeably with exoskeletons. However, there is a difference between the two. According to Herr, the purpose of orthosis is to assist those with pre-existing pathologies, contrary to exoskeletons which augment human capabilities, including healthy people [12]. Orthoses can also be passive [13] or active [14]. In the MIT labs, an active ankle-foot orthosis for drop-foot gait treatment has been developed [14].

Lower limb exoskeletons, when used as assistive devices, have two primary applications: (i) rehabilitation and gait training, or (ii) locomotion assistance to help perform daily life activities [15]. The control strategy, which specifies the way the exoskeleton moves and interacts with the user, is therefore based on the exoskeleton's application, as well as the condition of the patient using the device. *Trajectory tracking* is a type of control strategy, whereby an exoskeleton allows the patient to walk following a pre-defined gait trajectory pattern, often obtained from a healthy person. *Assist as needed*, is another control strategy whereby the support given by the exoskeleton is variable and dependent on the user's need. The level of assistance provided may be dependent on phase of gait, the level of effort exerted by the patient, and the stage a patient is in their recovery journey [15].

The control scheme is often a multi-level hierarchy, consisting of low, mid and high levels of control. The high level of control is responsible for user intention detection/event estimation. The mid-level is responsible for exoskeleton state transitions, based on the intention/event detected. An example of a mid-level controller is a Finite State Machine (FSM). The low-level is where user motion is tracked, and stability is ensured. Force, position, or impedance control are common low-level controllers [16]–[18]. Being at the top of the control hierarchy, intention detection and gait event estimation have a crucial contribution in the control and functionality of the exoskeleton and there have been numerous techniques used to analyse gait for their estimation.

Controlling exoskeletons is one for the most recent uses of gait analysis, which has already been used in various clinical and non-clinical applications for a long time. In clinical applications, gait analysis is used for rehabilitation assessment [19], and diagnosis of pathology [20]. In non-clinical applications, gait analysis is used in sports, for post-injury recovery monitoring [21] and performance evaluation [22], in security, for biometric identification and authentication [23]–[25], in safety, for elderly fall detection technologies [26], and in wellbeing, for emotional state identification [27].

Gait analysis involves measuring or estimating a range of parameters, including spatial-temporal parameters, EMG activity, kinematic, and kinetic parameters during walking or performing other locomotion activities [28]. To perform this analysis a range of wearable and non-wearable sensing modalities are used. Wearable sensors include inertial measurement units (IMUs) with accelerometers and gyroscopes, goniometers, electromyography (EMG), electroencephalographs (EEG), and foot pressure sensors. Non-wearable sensors include ground reaction force (GRF) plates and motion capture systems [28], [29].

Measurements from the wearable sensors are then processed to derive gait parameters. Researchers experimented with numerous algorithms for processing the sensor data. Examples include conventional thresholding algorithms to detect gait phases using angular velocity [30], musculoskeletal models to estimate intention using EMG [31], and numerous machine and deep learning techniques.

These gait analysis techniques have been reviewed, thoroughly compared and analysed in several published works in literature over the past few years. The advantages and disadvantages of multiple sensors used for gait phase detection have been reviewed, considering the number of phases that need to be detected, the location the sensor is placed and the computational algorithm used to process the sensor readings [32]. Wearable sensors have also been compared to conventional laboratory systems for analysing gait, as a protentional substitute to these systems [33]. Parameters of gait, machine learning algorithms and challenges in gait analysis for clinical and non-clinical applications were reviewed [28]. Some authors focused on reviewing a category of computational algorithms for gait analysis, such as intelligent predictive systems [34], or deep learning algorithms [29], while others focused on a specific category of algorithms and sensors, such as artificial intelligence using inertial sensors [35].

Despite these papers being published quite recently, between the years 2016 to 2020, none of them is solely focused on gait analysis techniques for the high-level control of the lower limb exoskeletons and orthoses. Before 2002, the number of papers published on exoskeletons where fewer than 30 per year and the cumulative number of papers published was lower than 500. By mid-2019, the cumulative number of papers was approaching 4000 [36]. With this exponential increase in research, it is desirable to have a systematic review focused on gait analysis for controlling lower limb robotics, deploying intelligent algorithms and techniques in particular.

Machine learning (ML) algorithms have multiple advantages that encourage their use over conventional gait analyses methods. Gait is temporal and the relationship between its parameters is non-linear. ML algorithms are capable of mapping relationships between inputs and outputs of non-linear systems [37]. When compared to conventional methods and heuristics used for analysing gait, ML algorithms are better at handling data variability. This is particularly important when analysing pathological gait which exhibits high levels of inter and intrasubject variability [38] ML implementations resulted in predictions with higher accuracy [38]–[40], as a consequence reducing torque prediction error [41]. They have had lower prediction time errors [38]. ML algorithms have also demonstrated adaptability, as they were able to form predictions under dynamic speeds [41] Furthermore, they shorten the time for tuning controller parameters

compared to manual tunning. The tuning of the parameters of the exoskeleton controller when used by different patients is necessary to accommodate for variations in patients' gait trajectories and strength capabilities, leading to more effective rehabilitation [42]. Some ML algorithms obviate the need for hand-crafted, or expert-selected features [43].

The numerous advantages of ML algorithms and their increased use were the impetus for this review paper, which will focus on research that has used intelligent algorithms (machine and deep learning), for the analysis of gait for the control or the potential control of active lower limb exoskeletons and orthoses. This paper will discuss the different gait parameters and features current researchers are detecting to be used for those robotic devices as well as the different sensors they have included in their designs. The information is organised into five sections. Section II of the paper will present background information on the topics reviewed. Section III will elaborate on the research methodology adopted rationalising the criteria by which the papers have been included or excluded. Section IV will include a review of the included papers. The papers are organised into subsections based on the parameter they are detecting/predicting. Within these subsections, the papers would be further aggregated based on the type of intelligent algorithm used. Finally, Section V will have a discussion and conclusion.

II. BACKGROUND INFORMATION

A. GAIT FEATURES AND RELATED PARAMETERS

According to Whittle, gait is a technical terminology used to describe 'the manner or style' we walk in [44]. Multiple parameters are observed when studying or describing gait. These parameters often have normal ranges for healthy gait with variations due to several factors such as anthropometric parameters (i.e. age, height and limb lengths) [45]. Parameters for pathological gait often deviate from these ranges. Each of the parameters included in this section has been detected, predicted and analysed for the control of lower limb robotics by using different mechanisms and techniques.

1) GAIT PHASE

There are cycles of events that periodically repeat during gait. Each cycle has a stance phase, where the lower limb is in contact with the ground, and swing phase where there is no contact. The stance phase can be divided into four periods: (1) loading response: begins with heel strike, and is also known as initial contact, (2) midstance: when the foot is flat on the ground as a result of a dorsiflexion moment (3) terminal stance: when the heel begins lifting from the ground, and (4) pre-swing: marks the last period of contact with the ground before the foot is lifted into the swing phase. The swing phase is further divided into three more periods: (1) initial swing, (2) mid-swing and (3) terminal swing. In total, the number of phases in a gait cycle is seven. This sequence of events happens to the right and left foot alternatingly, resulting in the forward movement.

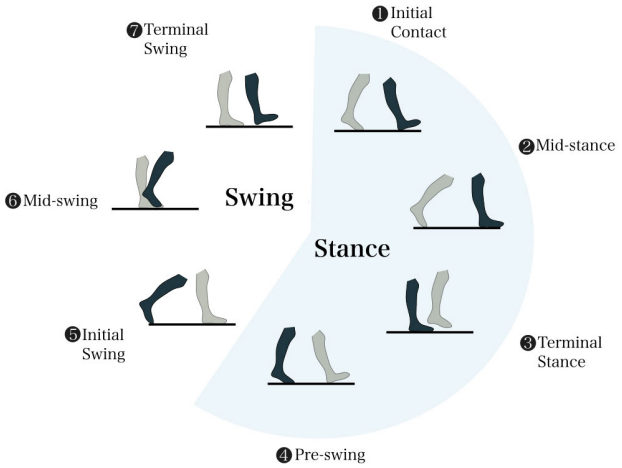

FIGURE 1. Phases in the gait cycle.

During a single gait cycle, there will be periods of double support, when both legs are in contact with the ground and single support, where one leg is in contact only [45]. Gait phases are part of the spatio-temporal parameters of gait [28].

2) JOINT ANGLE

The hip, knee and ankle joint angles periodically change every gait cycle. Their values are often measured in the sagittal plane, where the greatest movement is observed, compared to frontal and transverse planes [45]. The joint angles are considered a kinematic parameter of gait [28], and their first- and second-time derivatives, which are angular velocity and angular acceleration, are often observed/reported as well.

3) TORQUE / MOMENT

The moment of force refers to rotation caused by the application of force. The magnitude of the moment depends on the magnitude of the force applied and the shortest distance between the location of the force's application and a fulcrum/pivot. This distance is also called lever arm. There is a slight difference between moment and torque, moment results in bending and torque in rotating and twisting. Since the mathematical formula for both is the same, they are often used interchangeably [46]. In the case of biomechanics, a moment of force happens for instance when the muscles contract, causing the knee joint, which is an example of a pivot, to rotate. Internal moments can be passive due to the tension in soft tissue, or active due to the contraction of muscles (eccentric, concentric, and isometric contraction). External moments are due to external forces such as gravitational force. The rotational impact of these moments on joints is the net sum of all the individual moments, internal and external [45]. Moment is categorised as a kinetic parameter of gait [28].

4) LOCOMOTION MODE

Locomotion modes refer to several physical activities such as ground-level walking, standing up, sitting down, ascending and descending a slope, ascending and descending a staircase.

5) INTENTION

Intention in the field of human robot interaction has been defined as ''the need for the robot to have knowledge of some aspect of the human's planned action in order for the robot to appropriately assist toward achieving that action [47]''. Intention can be measured at the central nervous system level based on the brain's electrical activity, or at the peripheral nervous system level based on the muscle's electrical activity or based on interaction forces between the human and robot which can be measured with force sensors. Intention can have discrete states, where it can be used to trigger the start of a certain movement or transition between discrete control modes, or continuous states such as the desired position trajectory [47].

The two most common neural correlates reported by researchers for measuring intention from the brain are Movement-Related Cortical Potentials (MRCP) and Event-Related Desynchronization (ERD) [48], [49]. These neural correlates can be measured using electromyography (EEG). MRCP, first discovered by Kornhuber and Deecke, has multiple components including Bereitschaftspotential (BP). It begins around two seconds before the start of voluntary movement [50]. Meanwhile, significant ERD was observed to happen one second before movement initiation. ERD involves the reduction of spectral power of the alpha and beta bands, which have frequencies in the ranges of 8 to 13 Hz and 14 to 30 Hz respectively [51]. Two other neural features have been listed in He et al review paper on existing brain-machine interfaces used for lower-limb exoskeletons and orthoses control which are the rate of neuronal firing and Steady-State Visual Evoked Potentials (SSVEPs) [52].

Similarly, muscles are effectors to these commands, contracting as a result. Muscle electrical activity can be measured via surface electrodes, and voluntary activity initiation can be detected shortly before the joint torque. This time delay between the activation of a muscle and the generation of force is referred to as electromechanical delay [53].

B. MACHINE LEARNING ALGORITHMS

An algorithm is a list of procedures to transform an input into an output. When the procedures are unknown, thus cannot be explicitly programmed, it is possible to approximate the transformation using machine learning algorithms. Machine learning algorithms approximate the procedures of transformation by learning patterns between inputs and outputs. The patterns are learned by being exposed to large amounts of data in a specific subject domain. Learning is achieved when a pre-selected performance metric is optimised, such as the accuracy of predicting the output. Machine learning algorithms can be broadly categorised based on their style of learning [37]. The three main categories are supervised, unsupervised and reinforcement learning. Supervised learning algorithms require input and target output data. This type of learning involves continuously comparing the algorithm's generated output with the target output until the error between both is minimized [54]. Meanwhile, unsupervised learning doesn't require target output data. The algorithm attempts to find inherent patterns within the structure of the data [55]. Reinforcement learning also doesn't require target output data. It learns via a reward system [56]. Some of the machine learning algorithms include:

1) SUPPORT VECTOR MACHINE

Support Vector Machine (SVM) is an algorithm used for both classification and regression problems. First developed by Boser *et al.* [57], this supervised machine learning algorithm can separate linearly separable classes or features with a hyperplane. If for instance two classes can be separated by a linear line known as hyperplane, as in Fig 2, the optimal hyperplane is chosen to be the one that maximizes the distance between itself and the classes. The objective is to maximize the margin. If the classes are not linearly separable, they can be transformed into higher dimensions where they are linearly separable, or kernels can be used [57]–[60].

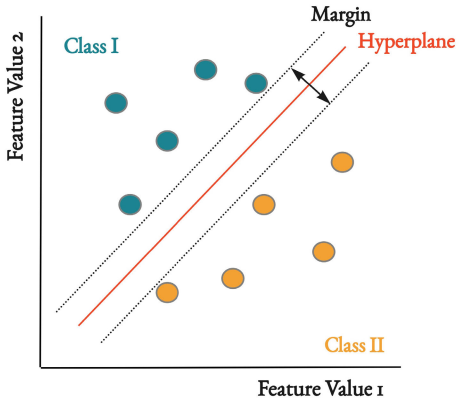

FIGURE 2. Support vector machine.

2) DECISION TREES

Decision trees are another type of supervised machine learning algorithms used for classification. They have a hierarchical tree-like structure starting with a root node. Each node is divided into multiple branches with attributes. These nodes are referred to as 'impure' and continue dividing based on the attribute's value until they reach the leaf node, an indivisible 'pure' node that represents a single class [60], [61]. ID3 [62] and C4.5 [63] are examples of popular decision trees.

3) NEURAL NETWORKS

Neural networks are connectionist networks, heavily inspired by the neurons of the brain [64]. The history of neural networks began with McCulloch and Pitts mathematical approximation of a neuron in 1943 [65], followed by Rosenblatt perceptron in the 1960s [66]. Neural networks consist of input, hidden and output layers. Each layer contains nodes, also called neurons. A single node in the hidden layer receives an input value from the previous layer. The node performs a non-linear mathematical operation and outputs an activation value. The mathematical operation is known as an activation

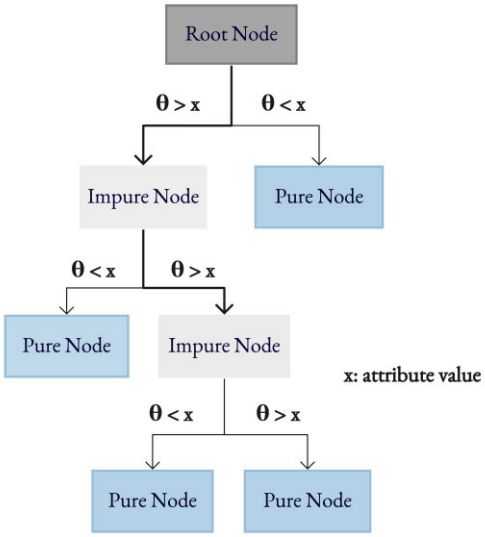

FIGURE 3. Simplified decision tree.

function such as a sigmoid function or tanh function. The activation value of this node is dependent on the input value, and the weighting to the node. The values of the weights are adaptive and change as the neural network is learning. If the input influences the generation of the output, a high weight is chosen, leading to a high activation value. Otherwise, a low weight is chosen. The multilayer perceptron (MLP) is a fully connected feed-forward neural network, where a node in a particular layer is connected to all the nodes in the previous layer and all the nodes in the preceding layer. Nodes within the same layer are not connected. This topology allows for parallel computations [60], [67], [68].

The radial basis function neural network (RBFNN) is another type of neural network. It differs however from MLP as it can have only one hidden layer. The mathematical computation at the nodes is also different. The nodes calculate the Euclidian distance between the input and pre-defined prototypes, which can be pre-set using an unsupervised algorithm such as the k-Means algorithm. Once the Euclidian distances have been calculated, a nonlinear Gaussian function is used as the activation function to calculate the output. The closer the data point is from the prototype, the greater its influence on the output, since the output of the Gaussian function would be close to one. The further away the data point is from the prototypes, the lower its influence on the output since the output of the Gaussian function would be close to zero [69].

Both of the aforementioned algorithms are supervised learning algorithms and are parametrized by weights, therefore, the values of these weights are selected to maximize the performance. The backpropagation algorithm, among others, is used for updating the values of the weights. It starts by measuring the error between the output of the algorithms compared to the target output. The errors computed, also referred to as cost, could be the cross-entropy error or the squared error. Afterwards, the derivative of the error with respect to the chosen weights is calculated. The objective is to minimize this error, and this is achieved by updating the weights based on the calculated derivative with every iteration until the error is minimized and satisfactory performance is attained. This process is also referred to as gradient descent, which is a type of optimization [70].

4) DEEP NEURAL NETWORKS

Deep feedforward neural networks are essentially neural networks with many hidden layers. The number of hidden layers determines the model's depth [71].

Convolutional neural networks (CNN) are a type of deep neural network that commonly uses 2D images as input data. The CNN has a kernel, that is smaller than the size of the original image. This kernel is scanned across the image performing a mathematical operation, the convolution operation, between the kernel and a portion of the image. This results in the formation of the next layer in the network also called feature map. Feature maps are analogous to hidden layers in ANNs. But unlike hidden layers in ANNs which have nodes that connect to every single input, in CNNs, a group of inputs the size of the kernel would be mapped to a single point on the feature map. This is one of the special features of CNN referred to as sparsity of connections. The sparsity of connections due to convolutions causes a reduction in the number of parameters in the model, thus a reduction in the memory storage space and the computational power required. Another special feature of the CNN algorithms is parameter sharing. To produce a single feature map, the same set of weights are used across the entire image. Weights are only changed when producing feature maps that extract different features. In addition to convolution layers, there are also other pooling layers. After several alternating convolution and pooling operations, the final feature map is unrolled to a fully connected hidden layer to generate the output [71], [72].

While CNNs are more well suited for 2D input data, there is another category of deep learning algorithms that works better with sequential data that are 1D, which are recurrent neural networks. Recurrent neural networks (RNN) have recurrent connections whereby previous outputs are used for the calculation of current output. Long short-term memory (LSTM) algorithm is a type of gated RNN. Its architecture consists of cells with an input, output and forget gate. LSTMs have the capability of learning long term dependencies, meaning that they can generate output depending on input data that happened much earlier in time [71].

III. METHODS

A. RESEARCH IDENTIFICATION

We have conducted a systematic review. This review is a 'systemic' way of exploring existing literature. It starts with choosing a set of keywords, along with Boolean operators, to try and extract only the most pertinent papers in literature. Since our focus is to review papers that implemented intelligent machine learning algorithms for gait analysis to be used

with lower limb exoskeletons and orthoses, the choice of keywords should reflect the topic. They should be general enough not to miss applicable literature and encompass the varying techniques, sensors and terminology researchers use in their research but restrictive to eliminate irrelevant research. The keywords we have chosen are:

(exoskeleton OR orthosis OR orthotic) AND (gait OR locomotion) AND (recognition OR classification OR prediction OR intention OR selection OR detection OR discrimination OR partitioning OR segmentation OR estimation) AND (''machine learning'' OR ''deep learning'' OR ''artificial intelligence'' OR ''neural'' OR ''fuzzy'').

B. DATABASES FOR RESEARCH EXTRACTION

The aforementioned keywords have been used to extract papers available in two databases: IEEE and SCOPUS. Initially, PubMed was also included but no relevant papers appeared in the search.

C. INCLUSION AND EXCLUSION CRITERIA

In addition to the keywords, an inclusion and exclusion criteria has been used to further filter the results. Research published between the years 1989 to May 2020 written in the English language were included. Results were limited to journal and conference papers only. There were a few studies on SCOPUS were the full-text paper was not available or inaccessible by us, hence were not included. The total number of papers identified with this inclusion and exclusion criteria was 226 papers. Afterwards, duplicate papers available on both databases have been removed, reducing the papers down to 172. These papers have been analysed based on abstract only, manually removing less relevant or irrelevant papers i.e., the scope of these papers have no significance to our review. Some reasons that resulted in the exclusion of papers include the use of prostheses rather than orthoses or exoskeletons, upper limb rather than lower limb robotics, and absence of intelligent machine or deep learning algorithms. Results were further limited to research articles excluding conference papers. 41 out of the 64 full-text articles that we assessed for eligibility were included in this review. We have reviewed the full text of these papers focusing on the parameters the researchers are considering, the intelligent algorithms they used, the sensing modalities, the types of subjects they have tested/trained their algorithms on and the overall performance of their systems. This process is visually illustrated in Fig 4.

IV. RESULTS

In this section, the 41 papers that met our inclusion/exclusion criteria will be reviewed. The aspects that will be reviewed are the performance of the algorithms, the data used for training and validation of the algorithms, and the signals/sensors used to obtain the predictions. The parameters will be discussed in the following order: (1) gait phase, (2) locomotion mode, (3) trajectory and joint angle and (4) torque and moment.

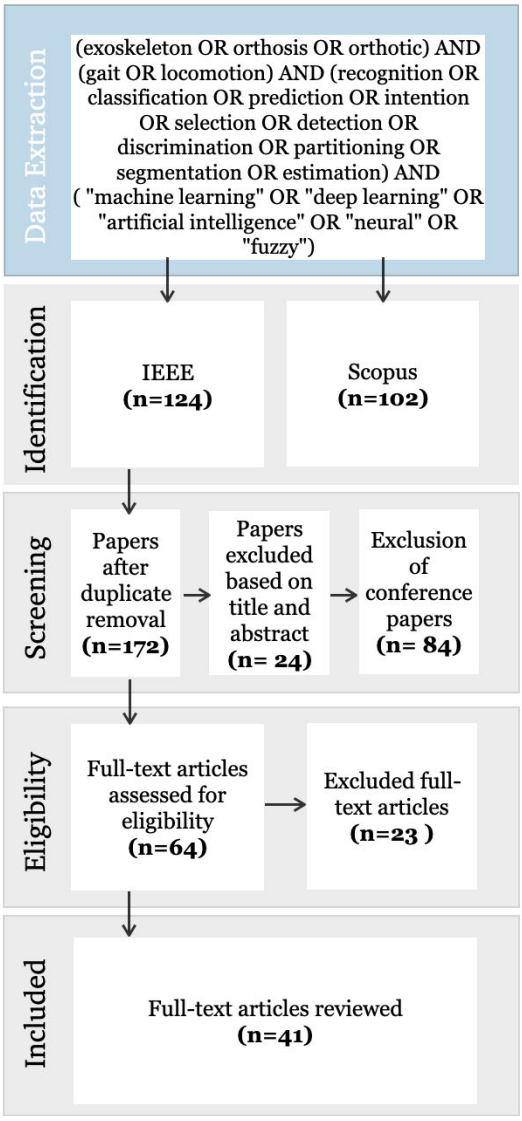

FIGURE 4. Flowchart on the methodology of article selection.

A. GAIT PHASE

The magnitude of assistive torque provided by the active exoskeleton or orthosis may vary according to the phase of gait [41], thus detecting some or all phases is a desideratum. A wide variety of wearable sensors have been used for this, as well as a plethora of algorithms. Furthermore, the granularity of the phase detection varied, from as low as two phases up to eight phases. This section will include a list of machine learning algorithms used for gait phase detection. The identified phases and the overall performance have been discussed in detail.

1) NEURAL NETWORKS

A multilayer perceptron neural network (MLPNN) is implemented by Jung *et al.* [39], to detect two gait phases: stance and swing. These phases are used to control their exoskeleton ROBIN-H1, designed for the rehabilitation of stroke patients. Pitch orientation and angular velocities were measured by

several sensors and were used as input to the MLP. Ground truth labels were obtained using force plates. The MLP had one hidden layer with growing nodes that increased from 5 to 50, and the MLP was optimised using the back-propagation algorithm. To analyse performance, classification success rate (CSR) was used. CSR accounted for three types of errors: early classification, delayed classification and erroneous classification. The authors considered erroneous classification error the most dangerous for robotic control and a potential cause of injury. Offline and online tests were conducted based on data from healthy subjects. The average CSR rate for the offline test was 97.75%, higher than online tests which scored 90.75% on average.

An MLPNN is implemented by Ma *et al.* [73], as a comparison to the kernel recursive mean square method (KRLS), to detect four phases of gait: heel strike, flat foot, heel off, and swing. The average classification rate of the MLPNN for 3, 5, and 10-fold cross-validation were 83.17%, 82.42%, 83.23%. The MLPNN had a lower performance compared to KRLS, by 2.33%, 3.62%, and 3.04% of KRLS's classification rate for 3, 5, and 10-fold cross-validation.

A neural network is implemented by Kang *et al.* [41] to estimate the percentage of the gait cycle, for controlling a bilateral hip exoskeleton. Instead of having discrete phases, gait was considered a continuous variable and the percentage of gait phase was detected with their model. The authors experimented with different combinations of sensors to train a neural network with one hidden layer and 20 nodes. They found that using all sensors combined resulted in greater error than using the hip encoder and thigh IMU only. This may be because of the simple architecture of the model used. Three models were evaluated: a generalized/independent model (trained on data from multiple users and tested on data from an unseen user), a user-specific/dependent model (trained on data from a single user and tested on unseen samples from that user), and a semi-dependent model (trained on data from multiple users and tested on unseen samples from one of the users it initially trained on). The three models were compared to a time-based estimation (TBE) model that uses FSRs, under varying gait speeds. For steady-state speeds, there wasn't a significant difference in performance, and the generalized model had the highest error even compared to TBE. However, under dynamic and extrapolated speed dynamic movements, the user-specific and semi-dependent models had higher accuracies compared to TBE, reducing estimation error by 23.4% and 26.3% respectively. Enhanced estimation caused the torque generation error to decrease by 32.4% ($p < 0.05$) for the dependent model and 40.9% ($p<0.05$) for the semi-dependent model. The best performance was for the semi-dependent model.

An adaptive neural-fuzzy inference system (ANFIS), which is a combination of Takagi-Sugeno fuzzy inference system and neural networks, is implemented by Hua *et al.* [74] for detecting two phases: stance and swing. Their objective was to develop a lower limb exoskeleton that withstands lifting of heavy loads. Predictions utilized plantar pressure readings and their first and second derivatives. A trapezoidal membership function was used. The authors demonstrated the model's generalization potential as they have segmented gait phases under various locomotion modes.

An MLPNN is implemented by Nazmi *et al.* [75], to detect gait phases: stance and swing using EMG signals. Two types of optimization algorithms have been compared. One achieved optimization in shorter duration, the scaled conjugate gradient (SCG) algorithm, and another resulted in higher accuracy and lower MSE, the Levenberg-Marquardt (LM) algorithm. Numerous features have been derived from the muscle activity for training the neural network including the use of mean absolute values (MAV) only, use of mean absolute value and waveform length (group 1), and use of mean absolute values, waveform length, RMS, SD and integrated EMG (group 2). Using the LM optimization algorithm, the accuracy using MAV features was 78.6%, for group 1 features was 82.3%, and for group 2 features was 87.4%. This indicated that using the greatest number of features lead to more accurate predictions.

A backpropagation neural network (BPNN) is implemented by Zhang *et al.* [76] to detect five phases of gait. The authors evaluated the effect of variations in the load carried by the users on the EMG activity, and the ability of an algorithm trained on data from users carrying one load level to perform accurate predictions when tested on data from users carrying multi-load levels. EMG data has been collected from users carrying multiple loads as a percentage of their masses (0%, 20%, 30%, and 40%) while walking on a treadmill at three different speeds. The authors found out that intra-load testing, which is training and testing a model using data from users carrying one load level, had higher accuracy than inter-load testing, which is training a model using data from users carrying one load level and testing it using data from users carrying another load level. This proves that muscle activity changes when varying the loads, and stresses the importance of training the algorithm with data from multi-load conditions to maintain the performance of the exoskeleton in various conditions.

2) DEEP NEURAL NETWORKS

A long short term memory algorithm and deep neural network (LSTM-DNN) is implemented by Zhen *et al.* [77], for the detection of two phases: stance and swing. The detection was based on acceleration signals obtained using an inertial measurement unit. The LSTM had 36 units with its output feeding into a DNN. The LSTM-DNN was tested under three pre-defined speeds, obtaining accuracies greater than 91.8% and F-scores greater than 92%. The LSTM model on its own had lower performance, with accuracies greater than 86.8% and F-scores greater than 86.4%.

A deep memory convolutional neural network (DM-CNN) is implemented by Wang *et al.* [78] to detect four phases of

gait, using foot pressure sensors and IMUs. Phase classification using the multi-modal approach (i.e., training the model on data from multiple sensors) achieved a higher performance than using the single-mode approach (i.e., training the model on data from a single sensor). Also, classification with acceleration signals alone was better than with pressure signals alone.

A type of recurrent neural network (RNN), called non-linear autoregressive with external inputs (NARX), is implemented by Jung *et al.* [39]. The performance of NARX was slightly lower than the MLPNN, with an offline CSR of 97.05%, and an online CSR of 91.93%. The NARX however, had fewer unstable regions, which are oscillations in the output, compared to the MLPNN. According to the authors, segmenting the data into individual strides for training may have resulted in discontinuities in the gait pattern, affecting the performance of NARX.

3) DECISION TREES/RANDOM FOREST

A logistic model decision tree (LMT) is implemented by Farah *et al.* [79], for the detection of four gait phases: loading response, swing, terminal swing, and push-off using knee angles, thigh angular velocity, and acceleration. The chosen LMT model was a J-48 decision tree, with terminal nodes performing a logistic function. The criteria for node splitting of the C4.5 decision tree was followed. Its size was 1643 containing 822 nodes. The authors also included a transition sequence validation and correction algorithm (TSVC) post-classification, for the removal of erroneous or misclassifications. This increased the training and validation accuracy which were 98.76% and 98.61% respectively. The F-score for the validation set was 0.97. It was noticed that a large proportion of false negatives were due to transition periods during the phases.

A random forest (RF) algorithm is implemented by Pasinetti *et al.* [80] to detect two phases of gait: stance and swing, using time of flight cameras. The authors had the cameras embedded in two crutches, that need to be used when walking with the exoskeleton. Each one of the crutch cameras monitors the contralateral leg. The depth images collected by the camera are processed to separate the leg and floor from the environment. A plane detection algorithm identifies the floor's surface which is used as a reference for measuring distances between it and other objects, i.e., foot. The percentiles of those distances are used as features for classification. Two variations of algorithms have been implemented, a random forest (RF) comprised of decision trees, and a sigma-z random forest. Sigma-z RF is a variation of RF, as it accounts for uncertainties such as measurement error, and for variances in the data collected that can occur if there is similarity/overlap between features of separate classes. Sigma-z outputs a classification, in addition to a confidence value for that classification. A trade-off between classification accuracy and the number of unclassifiable samples was evident, and it depended on the choice of admittance threshold. The RF and sigma-z RF had accuracy values of 81% and 87.3%.

4) FUZZY LOGIC

A Fuzzy logic algorithm is implemented by Chinimilli *et al.* [81] to detect four gait phases. Their goal was to create an adaptive virtual impedance control for a knee exoskeleton. Ground contact forces measured with smart shoes were input to a fuzzy logic algorithm comprised of partial trapezoid and triangular membership functions. The classified gait phase, in addition to the locomotion mode (will be further described in the next section), were used as inputs to a gaussian mixture model (GMM) that outputted appropriate stiffness and damping ratio for the control of the exoskeleton. While the classifier's performance has not been recorded, the performance of the automatic impedance tuning that relies on the outputted gait phase and locomotion mode has been assessed in comparison to constant impedance and finite state machine. The assessment involved measuring the EMG of the vastus medial, in addition to the step length and cadence using a motion capture system. The automatic impedance control showed desirable results, decreasing the EMG activity level, shortening the step length and increasing the cadence with respect to the two other control modes.

Fuzzy logic is implemented by Chen *et al.* [82], for the detection of four phases using foot pressure data. Their exoskeleton, HEXO, is controlled using hybrid control: adaptive impedance control (AIC) in stance phase and active-disturbance rejection control with fast terminal sliding mode control (ADRC-FTSMC) in swing phase. The fuzzy logic algorithm for phase detection had a sigmoid membership function.

A fuzzy logic algorithm is implemented by Huo *et al.* [83], for gait phase detection. E-ROWA is an exoskeleton that supports walking by generating appropriate torque according to the phase of gait. The authors also detect locomotion modes, which is discussed in the following section.

5) K-NEAREST NEIGHBOUR

The k-nearest neighbour (KNN) method is implemented by Chen *et al.* [84], to detect 8 gait phases. The recognition was based on multiple sensors including joint angle sensors that measure the angle of the hip, knee, and ankle joints, and plantar pressure sensors.

A KNN is implemented by Wang *et al.* [78], for the detection of four gait phases. KNN's performance was lower than three other algorithms, DM-CNN, N-HMM, and HMM. Its accuracy was 88.5%, 8.6% below the highest performing algorithm, while precision and recall values were 81.5% and 82.5% respectively.

A KNN is implemented by Zhen *et al.* [77], for the detection of two gait phases. They've experimented with seven values of K, ranging from 2 to 30, and have set the distance parameter to be the Euclidean distance. The algorithm's performance has been tested at three walking speeds.

The KNN had the worst performance compared to LSTM-DNN, LSTM, and SVM. Its accuracy ranged between 69% and 76% while its F-score between 70% and 77%.

A KNN is implemented by Zhang *et al.* [76], for the detection of five gait phases. The KNN algorithm had a lower performance than BPNN.

6) HIDDEN MARKOV MODEL

A hidden markov model (HMM) is implemented by Manchola *et al.* [40], to detect four gait phases using a single IMU placed on the instep of the foot. The classification with a HMM utilised gyroscope signals in the sagittal plane, instead of acceleration signals that require a Kalman filter to address the issue of drift. The Baum-Welch algorithm was used for model training and the Viterbi algorithm for gait phase recognition. Two types of trainings have been performed: inter-subject/subject-specific training (SST), were the algorithm was trained on data from a single user then tested on unseen samples from that user, and inter-subject/standardised parameter training (SPT). For healthy users, SPT involved training the algorithm on all healthy users and testing it on unseen samples of a one of those healthy users. For patients, the algorithm was trained on healthy users but tested on a patient. SST had higher accuracy values than the SPT, and this difference was more pronounced for the healthy subjects than for the patients. The SST accuracy was 81.44% for healthy users and 78.06% for patients, meanwhile, the SPT accuracy was 76.91% for healthy users and 76.36% for patients. Despite both training approaches, the accuracies for HMM were still higher than the threshold-based algorithm also implemented, which is a finite state machine that classifies gait based on detecting peaks, troughs and zero-crossings of accelerometer and gyroscope signals.

A HMM and N-HMM were implemented by Wang *et al.* [78], as a comparison to DM-CNN. Both the N-HMM and HMM had lower accuracies than DM-CNN model, scoring 96.2% and 92.3% respectively.

7) SUPPORT VECTOR MACHINES

A SVM is implemented by Ma *et al.* [73], as a comparison to the kernel recursive least-square method (KRLS) and MLPNN, to detect four gait phases. The SVM had a Gaussian kernel function and was optimised using particle swarm optimization. The SVM's accuracies for 3, 5, and 10-fold cross-validation where 83.00%, 82.69% and 83.29%. Its performance was lower than the KRLS.

A SVM is implemented by Zhen *et al.* [77], for the detection of two gait phases. Four kernel functions were used: linear, rbf, sigmoid and poly with the rbf kernel resulting in the highest performance. The SVM was outperformed by the LSTM-DNN and LSTM model. It was slightly higher than the kNN.

A SVM was implemented by Zhang *et al.* [76], and compared to BPNN, KNN, and SVM. KNN and SVM demonstrated lower performance than the BPNN.

8) PRINCIPAL COMPONENT ANALYSIS

A probabilistic model is implemented by Tanghe *et al.* [85] for the prediction of four phases of gait before they occur. The authors implement a probabilistic principal component analysis (PPCA) model which predicts initial contact, flat foot, heel off, and toe off events along with joint trajectories. The training dataset was based on healthy participants walking without an exoskeleton and validated on two data sets: one for healthy participants walking without an exoskeleton and another for healthy participants walking with an exoskeleton. For the reported results, zero-error means the phase was predicted 0.2s before to the actual event. 9ms was the maximum median error for the exoskeleton-free validation dataset across all four phases. The median errors for the dataset involving the exoskeleton were higher, reaching 15ms for initial contact, and 33ms for toe-off. Heel off was the most challenging phase to predict.

9) KERNEL RECURSIVE LEAST SQUARE METHOD

A kernel recursive least square method (KRLS) is implemented by Ma *et al.* [73], for gait phase detection, using the knee and hip joints angle as input. The accuracies of gait phase classification for 3, 5, and 10-fold cross-validation where 85.49%, 86.04%, and 86.26%.

B. LOCOMOTION MODE

Identifying the locomotion mode is essential for robotic devices that provide assistance with daily life activities. This is because each activity requires specific assistive requirements, and identifying the mode allows for smooth transitions between the different activities. Locomotion modes can be classified into static or dynamic modes. The main static locomotion modes are sitting and standing. The main dynamic locomotion modes are straight level walking, ascending stairs, descending stairs, ascending slope, and descending slope. Some authors detect mode transitions, such as sitting to standing or level walking to ascending etc. Often, identification of locomotion mode is performed in conjunction with gait phase detection, pre-or post-identifying the current phase.

1) NEURAL NETWORKS

A BPNN is implemented by Song *et al.* [86], for locomotion mode detection. They detected 4 static, and 11 dynamic modes, a total of 15 locomotion modes including sitting, standing, level walking, level walking with weight etc. They used IMUs and foot pressure sensors to acquire signals, from which they extracted time domain, frequency domain and energy features. A total of 141 features have been extracted, including mean, variance, correlation coefficient, wavelet energy entropy, SMA, Fourier series and maximum values. Some features are more suited for classifying static modes such as leg angles, and others for dynamic modes. Three neural networks were developed with three layers each. The first to classify whether the mode is static or dynamic and

contained 5 input, 25 hidden, and 1 output node. Depending on the outcome, a static mode or a dynamic mode neural network followed. The static neural network constituted of 20 input, 100 hidden and 1 output nodes while the dynamic had 40 input, 200 hidden and 1 output. The authors found it easier to classify dynamic modes, as they have larger inherent differences in their patterns than static modes. An example of common confusion is between standing and sitting with a load. For single-mode classification, the overall accuracy was 98.28%. The accuracy of multi-mode classification, which involves transitioning between modes was lower.

An ANN is implemented by Islam and Hsiao-Wecksler [87], to detect: level walking, ascending stairs/ramp, and descending stairs/ramp, for controlling their Portable Powered Ankle-Foot Orthosis (PPAFO) using IMU and foot pressure sensors. Calibration was performed with every step due to drift, specifically at the zero-acceleration stage (mid-stance). The foot pressure sensors assisted in identifying mid-stance for calibration.

The input of a three-layer neural network were six tapped delays of vertical foot velocity and angle measurements, both derived from IMU. There were 10 nodes in the hidden layer and 3 nodes in the output layer. The authors performed subject-specific training and their accuracies were between 97.8% and 100%. They have also measured the time required to detect a transition, as a percentage of the gait cycle. This represents how much of the gait cycle elapsed before a mode transition is detected. Mode transition were detected in the swing phase of the transitioning step, within 28% of the gait cycle for the stair mode and 16% of the gait cycle for the ramp mode.

Backpropagation neural network (BPNN) and radial basis function neural network (RBFNN) are implemented by Wang *et al.* [88], to detect six locomotion modes with IMUs and plantar pressure sensors. The architecture of the BPNN and RBFNN consisted of 20 nodes for input, 12 nodes for hidden layer and 6 outputs. The BPNN's performance was superior to RBFNN, with an accuracy of 93.3% compared to 91.2%.

2) SUPPORT VECTOR MACHINE

A support vector machine (SVM) is implemented by Wang *et al.* [88], to detect six locomotion modes. The SVM outperformed two algorithms, the RBFNN and BPNN, achieving an accuracy of 96.5%. When the linear and polynomial functions were compared as choices of kernel functions, the linear kernel resulted in better performance.

An SVM (with gaussian kernel) is implemented by Villa-Parra *et al.* [89], for locomotion intention prediction based on EMG. The authors used muscle activity of the trunk and compared it to that from the lower leg, for predicting the intention to perform several locomotion modes such as flexion-extension of the knee, standing up, sitting down etc. The authors reported accuracies ranging between 76%-83% and 71%-77% for lower limb and trunk muscles respectively. The impetus for comparing the accuracy from the different types of muscles was to measure how comparable trunk muscles were to lower limb muscles in their ability to make accurate locomotion intention predictions, and if they can be used as an alternative to lower limb muscles which are often affected by pathologies or weakness for patients with preserved trunk muscle activity.

An SVM is implemented by Goh *et al.* [43], as a comparison to a Spectral Representation Learning Model (SSRL) for the detection of four locomotion modes with EEG. Principle Component Analysis (PCA) and F-score (FS) were used for dimensionality reduction. SVM-PCA and SVM-FS performed worse than SSRL. SVM-FS still performed better than SVM-PCA.

3) DEEP NEURAL NETWORKS

Deep neural network (DNN) and convolutional neural network (CNN) are implemented by Hua *et al.* [74], for detection of 6 locomotion modes. They have experimented with several machine learning algorithms, including DT, DA, KNN, SVM, EM which were pre-processed with kPCA to reduce the dimensions of the input features. The deep learning algorithms outperformed ML algorithms, requiring a lower duration (20 ms) to perform the computation, and achieving 52% higher efficiency, without the need of kPCA. The authors implemented the stacked autoencoder DNNs, optimized with genetic algorithm particle swarm optimization (GA-PSO) and achieved accuracies around 99%. Prior to optimization, the accuracies where 97.2%.

A spatio-spectral representation learning model (SSRL) is implemented by Goh *et al.* [43], to detect four locomotion modes using EEG signals: level walking without an exoskeleton, level walking with an exoskeleton at zero, low, and high torque support modes. Inspired by the weight sharing feature of convolutional neural network, the authors implemented a SSRL with 3 hidden layers, that include a spatial layer, a spectral layer and a fully connected layer. Data from 27 healthy male subjects was collected from 20 EEG channels. The models were trained either with wide spectral frequencies (WS) which range from 1-42 Hz or prominent spectral frequencies (PS) which range from 8-30 Hz. They compared the SSRL with two other machine learning algorithms, random forest and support vector machines with radial basis function kernels. Also, the authors reduced the dimensionality of data for the latter two algorithms, using principal component analysis (PCA) or F-score (FS). The SSRL-WS had the highest accuracy, $77.8 \pm 1.8\%$. The accuracies of SVM-FS, SVM-PCA and RF-FS algorithms for the wide spectral frequencies where $74.3 \pm 1.6\%$, $64.3 \pm 1.8\%$, and $65.9 \pm 1.8\%$ respectively. The accuracies when using the prominent spectral frequencies were lower, but the algorithms still had the same order of performance, with SSRL achieving $72.9 \pm 1.7\%$, while SVM-FS, SVM-PCA and RF-FS achieved $70.2 \pm 1.6\%$, $54.8 \pm 2.0\%$, and $58.9 \pm 1.7\%$ respectively. The results showed that when comparing the dimensionality reduction algorithms, FS which relies on handcrafted features was better than PCA. However, using

TABLE 1. Gait phase.

Authors	Model	Phase Granularity	Performance Metric	Value of Performance Metric	Optimization Algorithm	Sensors	Sample	Purpose
Jung et al [39]	MLP (a) NARX (b)	2	CSR	97.75% (a) 97.63% (b) (offline) 90.75% (a) 91.93% (b) (online)	Back-propagation	IMUs absolute encoders incremental encoders force plates (for segmentation)	10 healthy (7 offline training + validation, 3 online validation)	Stroke patient rehabilitation
Kang et al [41]	NN	% of the gait cycle	RMSE (for semi-dependent model)	5.07 ± 0.49% (steady-state) 5.22 ± 0.81% (dynamic)	SGD optimizer with Nesterov momentum	absolute encoders (on actuators) IMUs (thigh and trunk) FSRs (for segmentation)	8 healthy (initial data collection) 10 healthy (for validation)	Bilateral hip exoskeleton
Hua et al [74]	ANFIS	2	-	-	-	Plantar pressure		heavy load lifting
Nazmi et al [75]	MLPNN	2	accuracy (group 2 features and LM algorithm) mean absolute time difference compared to FSRs (for unlearned data)	87.4% 35±25 ms (heel strike) 49±15 ms (toe-off)	Levenberg Marquardt (a) scaled conjugate gradient (b)	EMG (tibialis anterior, gastrocnemius medialis) foot pressure sensor (evaluation only)	8 healthy	-
Zhang et al [76]	BPNN (a) kNN (b) SVM (c)	5	accuracy	91.81 ± 3.69% (intra-load) (a) 69.42 ± 7.86% (inter-load) (a)	-	EMG (tensor fasciae latae, vastus medialis, semitendinosus adductor longus) Camera (for segmenting gait cycle)	10 healthy	-
Zhen et al [77]	LSTM-DNN (a) LSTM (b) KNN (c) SVM (d)	2	Accuracy (1 m/s velocity) F-score (1 m/s velocity)	91.8% (a) 86.8% (b) 69.0% (c) 71.0% (d) 92.0% (a) 86.4% (b) 70.0% (c) 72.3% (d)	AdaGrad	IMUs (thigh, instep, calf)	4 healthy	-
Wang et al [78]	DM-CNN (a) KNN (b) N-HMM (c) HMM (d)	4	Accuracy Precision Rate Recall Rate	97.1% (a) 88.5% (b) 96.2% (c) 92.3% (d) 95.9% (a) 81.5% (b) 95.5% (c) 92.0% (d) 94.5% (a) 82.5% (b) 93.5% (c) 90.5% (d)	Back-propagation	pressure sensors IMUs (calf and thigh)	10 healthy	-
Farah et al [79]	DT+TSVC	4	Accuracy (validation set) F-score	98.61%	-	Computer-Assisted Rehabilitation Environment	30 healthy (training) +	Stance-control knee-ankle-foot orthoses for knee-

TABLE 1. *(Continued.)* **Gait phase.**

			(validation set)	0.97		(CAREN-extended) containing: Force-plates Motion Capture System	12 healthy (validation)	collapse prevention
Pasinetti et al [80]	RF (a) Sigma-z RF (b)	2	Accuracy	81% (a) 87.3% (b)	-	time of flight cameras	4	walking in indoor/outdoor environments (with crutches)
Tanghe et al [85]	PPCA	4	Median Error Without exoskeleton With exoskeleton	<9ms (all events) 15ms (initial contact) 33ms (toe-off)	-	Vicon cameras split belt treadmill for GRF (for segmentation)	28 healthy (without exo) + 5 healthy (with exo)	Exoskeleton that uses feedforward allowing control modes to transition more smoothly
Chinimilli et al [81]	Fuzzy logic	4	-	-	-	smart shoes IMUs (thigh and shank + not used for gait phases) EMG (for testing only) Motion capture	3 healthy	Knee assistive device with automatic virtual impedance modulation
Chen et al [82]	Fuzzy logic	4	-	-	-	foot pressure sensors		Locomotion assistance using hybrid control
Huo et al [83]	Fuzzy logic	4	-	-	-	Foot pressure sensor (GRF) IMUs Absolute encoders (hip, knee, and ankle)	4 healthy	Walking assistance using hybrid power assistive control
Chen et al [84]	kNN	8	Correct rate of phase classification	95.32%	-	Joint angle sensor (hip, knee and ankle) plantar pressure sensor	10 healthy	Locomotion assistance full body exoskeleton
Mancholia et al [40]	HMM	4	accuracy (SST) accuracy (SPT)	81.44% (H) 78.06% (P) 76.91% (H) 76.36% (P)	-	IMU (instep) FSR per foot (reference and testing only)	18 (9 healthy, 9 hemipareti c)	exoskeleton for hemiparetic patients
Ma et al [73]	KRLS (a) SVM (b) MLPNN (c)	4	accuracy (10-fold cross validation)	86.26% (a) 83.29% (b) 83.23% (c)	-	goniometer (hip and knee joint) foot pressure sensor (for segmentation)	10 healthy	Walking assistance for paraplegics + rehabilitation of stroke patients

CSR = Classification Success Rate
RMSE = Root Mean Square Error
SST = subject-specific testing
SPT= subject standardised testing

SSRL obviated the need for handcrafted features and still performed better. Also, the spatial parameters of the network allowed to deduce the roles of the different brain regions in controlling gait, contributing to our understanding of the topographic organization of the brain.

4) FUZZY LOGIC

A fuzzy inference algorithm is implemented by Chinimilli *et al.* [81], to detect three modes: level walking, uphill and downhill walking. The algorithm relies on the detected heel strike (right leg) and knee angle derived from

IMUs on thigh and shank. The number of locomotion modes they've detected was limited by the experimental apparatus which involved a treadmill only.

A fuzzy logic algorithm is implemented by Parri *et al.* [90], to detect seven locomotion modes for the control of a hip orthosis. A threshold-based algorithm is first used to categorise whether a mode is static or dynamic using hip angles. If the mode is static, the mode is identified. Static modes include sitting, standing and the transitioning between the two. If the mode is dynamic, a fuzzy logic algorithm is used for its detection. The dynamic modes are classified into level walking, ascending and descending stairs. The classification is based on hip joint angles, and centre of pressure measured by sensitive insoles. A gaussian function is used as a membership function. The authors opted to avoid subject-specific training as they wanted to produce a generalized model, therefore the membership values were based on data from 6 subjects with varying speeds and assist modes. The effect of inter-subject variability had a noticeable impact on the decline of performance for one of the subjects which was taller than the others.

A fuzzy logic algorithm is implemented by Huo *et al.* [83] to detect five modes of gait. The Mamdani fuzzy inference system has been specifically implemented with bell-shaped curves as membership functions. While wearing the E-ROWA exoskeleton, four healthy participants were asked to walk under normal and simulated abnormal gait, with the simulated abnormal gait demonstrated by locking the flexion of one knee joint. Accuracies were greater than 97.7% for normal gait and 97% for abnormal gait. The authors reported the latency of detection (with modes detected at the start of the step rather than the end of it) was less than $32 \pm 8.3\%$ of a step.

5) RANDOM FOREST/DECISION TREE

Decision tree is implemented by Novak *et al.* [91], to decode intention of gait initiation and termination of gait, without the use of physiological signals. Instead, the authors used IMU and pressure insoles. Gait initiation is when a person in steady state begins walking. It is divided into two parts: onset which includes events that happen in preparation to toe-off, approximately 0.5 s before the foot begins to lift from the ground, and toe-off which is when the foot is fully lifted from the ground. Gait termination is when a person is walking and decides to stand still. In the last step before a person completely stops, the parameters of gait are altered thus it is possible to detect the intention to terminate gait during that step. Decision trees have been tested based on within-subject and subject-independent trials. Within-subject trials yielded better results than subject-independent trials. The use of IMU and pressure sensors separately and combined as input to decision trees have also been compared. For detecting gait termination, the IMUs were found to perform better. However, pressure insoles were still needed for gait termination detection, particularly for segmentation of gait cycles. For 80% of the within-subject classification trials, gait termination intention was predicted prior to the actual event. The results reported where based on offline testing. The usefulness of this research will be in assisting a user with their first step upon detection of their intention to walk or terminate this assistance when they desire to stop walking. The authors remarked that the effects of an assistive device, such as an active orthosis, on 'masking' intention is yet to be evaluated.

A random forest (RF) algorithm is implemented by Goh *et al.* [43], to detect four locomotion modes with EEG. Pre-processing involved dimensionality reduction using F-score (FS). RF-FS algorithm performed worse than the SSRL model to which it was compared.

6) MULTIPLE KERNEL LEARNING

Multiple kernel learning (MKL) algorithm is implemented by Zhang *et al.* [92], to decode intention for performing four locomotion modes using EEG. 64 channels of electrodes were used and placed according to the 10-20 international system. The modes were forward walking, stopping, turning left and turning right. The brain was segmented into 13 regions, and the algorithm has been tested on two participants, one with healthy gait and another with a spinal cord injury. The role of the brain regions was also studied, by looking at the weightings of the MKL parameters. The frontal and front-central regions, particularly, the MFC and RFC had the highest weighting indicating the largest role in intention/limb control. However, the exact precedence of those regions differed in the healthy and SCI participants, with the healthy participant having the highest weighting in MFC followed by the RCF region, while the SCI participant had the reverse order. Two experimental sets to evaluate the model were designed, the first consisted of a single session. The model had a 74.5% detection accuracy for the healthy participant and 68.4% for the SCI participant. Another experimental setup consisted of nine sessions over 30 days. The classifier was set to detect walking and stopping only. The accuracy was greater than 90% and the weighting of the regions changed with training, indicating cortical plasticity. The weighting and accuracy increased with the progression of the sessions. Also, out of the four modes classified, the stopping mode was detected with the greatest difficulty.

7) SPARSE DISCRIMINANT ANALYSIS

Linear discriminant analysis (LDA) is implemented by Gui *et al.* [93] to detect intention for four locomotion modes: stopping, level walking, accelerating, and decelerating. The authors relied on cognitive and peripheral signals. LDA relied on brain generated Steady-State Visual Evoked Potentials (SSVEP) as input features. The output of the LDA is used by a central pattern generator to generate the exoskeleton's trajectory. The recognition rate of steady-state (ROS) was 92.40%. The time delay, also called the duration of transient state (DOT), was 1.7 seconds. The authors discussed the effect of increasing the locomotion modes from four to eight on the quality of SSVEP, which reduced ROS to 70%. The transitioning between the four discrete modes was performed

using EEG, whereas continuous locomotion speed control was performed using EMG. EMG was the input to an admittance model and the reader is advised to refer to the paper for details on that.

Sparse discriminant analysis (SDA) is implemented by Lopez-Larraz *et al.* [94] to identify gait initiation intention. Their exoskeleton is intended to assist patients with incomplete spinal cord injuries. From the generated EEG signals which were cue-guided, event-related desynchronization (ERD) and movement related cortical potential (MRCP) features were derived to be used with their model, with SDA being also used for feature selection. The model was tested on data from 3 healthy participants and 4 SCI patients. The experimental protocol contained four parts: ''rest'', then ''preparation'', then ''attempt movement'' and ''movement''. The accuracy for decoding the intention of healthy users was higher than those with SCI, 88.44 $\pm$ 14.56% compared to 77.61 $\pm$ 14.72%. It was also observed that frequency ERD features where more commonly chosen over temporal MRCP features.

8) CANONICAL CORRELATION LEARNING

The canonical correlations algorithm (CCA), an unsupervised learning algorithm, is implemented by Zheng *et al.* [95] to decode intention for three motion patterns. The features the authors used are steady-state visual evoked potential (SSVEP). They have performed offline and online experiments. The offline experiments involved visual stimuli followed by intention classification. This experimental design relied on EEG. The online experiments involved both visual stimuli followed by performing physical motions that included squatting, walking then standing. This experimental design involved multimodal data as input features, including foot pressure and joint positions. Both experimental designs achieved a classification accuracy of over 90%.

C. MOMENT/TORQUE

Torque and moment are kinetic parameters of gait that have been detected with a few machine learning algorithms as follows.

1) NEURAL NETWORK

An MLPNN is implemented by Ma *et al.* [73], to predict hip joint assist torque to support the extension and flexion of the hip. To assist in extension, torque needs to be provided at two phases: heel strike and flat foot. To support flexion, torque needs to be supplied at two other phases: heel off and swing phase. The authors developed a generalised model, which was trained on one group and tested on another. When compared to the kernel recursive least-square method, the MLPNN's mean square errors were twice as large.

A radial basis function neural network (RBFNN) is implemented by Gui *et al.* [96], to output passive and active torques. This method is an alternative to the hill-type model, often used for deriving torque from EMG activity. The torques are input to a motion controller, the extended Slotine-Li, that controls an assist-as-needed exoskeleton. Two neural networks are used, one that uses motion states as input and outputs passive torque, while the other uses motion states in addition to processed EMG signals as input and outputs active torque. The first RBFNN is trained with the muscles relaxed until a satisfactory steady-state error level is reached. Subsequently, the second NN is trained while asking the subjects to perform voluntary active torque and keeping the parameters of the first NN constant. The outputs are compared against measurements with torque sensors. The authors calculated torque in swing phase only, due to the unavailability of force plates. The use of the Slotine-Li scheme obviated the need for the calibration of EMG signals. For 'activity-based neuroplasticity' to occur, the delay between estimated and actual torques need to be below 300ms. This has been achieved as the time delay ranged between 174ms and 305ms. In future work, the authors suggest using high density EMG.

A neural network is implemented by Xiong *et al.* [97], for internal joint moment prediction using EMG signals and joint angles. An elastic net was used to eliminate noise and redundant features in the input, preceding the neural network. This lowered the computational load and allowed for real time prediction. The data of 8 healthy subjects obtained from an online dataset was used to train the NN. The outputs were compared to joint moment values calculated via inverse dynamics, which the authors noted is a source of limitation since the calculated values do not account for the presence of errors between them and the actual internal torque.

An extreme machine learning neural network (ELM) is implemented by, Xiong *et al.* [98], to predict joint moments. A hill-muscle model is used to determine which features are necessary for the ELM to perform predictions. The authors were able to calculate moments for flexion and extension of the hip and knee, abduction and adduction of the hip, and the plantar and dorsiflexion of the ankle. The variance accounted for (VAR) was used to evaluate the performance. Results showed that using muscle activity, muscle actuate joint angles, and angular velocities (instead of joint angles and angular velocities) results in the best performance, with VAF of 89.67 $\pm$ 5.56%. Using EMG alone lowered VAF by 82.83%. This indicates the inadequacy of relying on EMG signals alone for joint moment calculation. The performance achieved without foot pressure sensors demonstrates that they are not needed.

2) KERNEL RECURSIVE LEAST-SQUARE METHOD

Kernel recursive least-square method (KRLS) is implemented by Ma *et al.* [73], to predict hip joint assist torque. It has been compared against MLPNN, with MLPNN performing worse than KRLS.

D. JOINT ANGLE AND TRAJECTORY

Joint angles and trajectories are considered a kinematic parameter of gait and have been primarily predicted using neural networks and principal component analysis.

1) NEURAL NETWORK

An artificial neural network (ANN) is implemented by Kutilek and Farkasova [99], to predict joint angles using cyclograms. The authors used a neural network trained with backpropagation to predict future joint angles. The inputs to the neural network were current joint angles (for a single joint), angular acceleration, weight, and age. They trained a separate neural network that uses inclination angles calculated using PCA, in addition to the angles of two joints as inputs. Hip-knee predictions were found to be more accurate than ankle-knee predictions. The neural network that uses inclination angles also performed better. In another paper published a year later, Kutilek and Viteckova [100], also use the 2nd moment of area (x-axis and y-axis) as additional inputs.

A radial basis function neural network (RBFNN) is implemented by Mazumder *et Al.* [101], to generate gait trajectories. The authors use joint angles derived from IMU signals, gait phases and stride times that are calculated based on EMG signals, and foot pressure sensors as input to the RBFNN. The model was trained based on data from 5 healthy subjects and is capable of adapting to the user's pace of walking and anthropometrics.

RBFNN and MLPNN are implemented by Lee *et al.* [102] for the calculation of joint angles, using EMG signals. Their focus was the use of joint angles of a healthy leg to predict the joint angles of a pathological leg with an orthosis, or even a prosthetic. Two neural networks have been used, an RBFNN which uses EMG signals from the rectus femoris to predict knee joint angles of the healthy lower limb and an MLPNN which uses the output of the RBFNN to predict the hip and joint angles of the pathological lower limb. The experimental setup included measuring joint angles during level walking, sitting and standing off a chair, with an average accuracy of 97.5% and an absolute average error rate of 0.25°.

A generalized regression neural network (GRNN) and BPNN have been implemented by Xie *et al.* [103] for the calculation of joint angles. EMG, hip joint angles, and plantar pressure were used as inputs. Their primary algorithm was the GRNN and was optimized with the golden-selection algorithm. The transfer function was a gaussian kernel. Wavelet denoising was also implemented since high frequency signals contribute to the instability of data affecting the output of the GRNN. Meanwhile, the BPNN was trained with the Levenberg-Marquardt algorithm. The GRNN had a shorter prediction time than the BPNN, 2.38s compared to 16.029s respectively, for very similar correlation coefficient values.

An Elman neural network is implemented by Wang *et al.* [104], to detect knee joint angles using EMG. The signals were recorded during leg extension exercises at various speeds, with and without load. A multilevel wavelet decomposition was performed followed by the calculation of the correlation dimension. The correlation dimension of wavelet coefficients (WCCD) was used with the Elman neural network. Since the neural network receives feedback, it has a memory component to it. The WCCD was compared against time-domain feature extraction algorithms, IEMG and RMS, and frequency-domain feature extraction algorithms, MNP. The RMSE was the lowest for the WCCD method. Furthermore, the Elman Neural network outperformed other algorithms, including BPNN, LSSVM, GRNN. The authors also reported that at higher speeds of the extension exercises the RMSE was larger. However, when comparing exercises with and without load under constant speeds, having load resulted in lower RMSE.

Three MLPNN are implemented by Gomes *et al.* [105] to generate trajectories for a lower limb orthosis. The first neural network performs inverse dynamic approximations, calculating torque variations. The second neural network performs an optimization to calculate the adapted step time. The third neural network calculates the trajectory that will be the input to the orthosis's position controller. The trajectories outputted by the third neural network include a value for position, velocity, and acceleration. Since the zero-moment point criterion is considered in this design, as well as the interaction forces between the user's limb and the orthosis, the user can voluntarily alter their walking pattern, such as increasing their speed while preserving the stability.

An autoencoder neural network (AENN) is used by Wu *et al.* [106], for the prediction of hip and knee joint trajectories. These generated gait patterns will be used by their lower limb robot SLEX and are based on the walking speed as well as 21 body parameters. A Gaussian regression process (GRP) with automatic relevance determination (ARD) is used to map the relationship between walking speed (desired) and body parameters to spatial-temporal features. Spatial-temporal features are used by the AENN which outputs joint trajectories for the knee and hip angle. This process allows for individualized gait trajectories based on the person's particular body parameters, allowing the sharing of the exoskeleton by multiple users.

2) DEEP NEURAL NETWORK

A recurrent neural network (RNN) is implemented by Boudali *et al.* [107] for hip and knee joint trajectory prediction during transitioning locomotion modes such as level walking and ascending stairs. The authors used the angular position and velocity of a cane, to predict the angular position of the contralateral foot. A RNN was used for dynamic mapping and was compared against the least square method, which performed static mapping. The RNN not only had better performance but was capable of producing predictions during mode transitions (i.e., not limited to predictions during steady state), which was a limitation of the least square method. Introducing the position and velocity of an arm to the model further lowered the RMS errors of the predictions which were 1.36° and 2.48° for the hip and knee joints respectively, for experiments involving intra-subject training. Accuracy was greater for intrasubject mappings than for inter-subject mappings.

TABLE 2. Locomotion mode.

Authors	Model	Locomotion Mode Number	Modes	Performance Metric	Value of Performance Metric	Optimization Algorithm	Sensors	Sample	Purpose
Song et al [86]	BPNN	15	sitting standing running level walking (multiple paces and with weight) etc. (refer to paper for exhaustive list)	accuracy (single-mode) accuracy (multi-mode)	98.28% 92.7% (group 1) 97.4% (group 2)	-	IMUs per leg (foot, calf and thigh) foot pressure sensors Vicon motion capture (for normalization and validation of sensors)	healthy	-
Islam et al [87]	NN	3	level walking ascending stairs/ramp descending stairs/ramp	accuracy	97.8% - 100%.	Lavenberg - Marquardt algorithm with Bayesian regularization	IMU (heel) foot switches	5 healthy	Powered ankle foot-orthosis with variable ankle actuation during swing
Wang et al [88]	SMV (a) BPNN (b) RBFNN (c)	6	standing level walking stair ascent stair descent slope ascent slope descent	accuracy	93.3% (b) 91.2% (c)	Trainlm for (a) and (b)	IMUs (right and left thighs and calf, waist) FSRs	5 healthy	-
Villa-Parra [89]	SVM	6	Standing up Sitting Flexion-extension of knee Level walking Resting while standing up Resting while sitting down	accuracy	76%-83% (lower limb muscles) 71%-77% (trunk muscles)	-	sEMG (biceps femoris. erector spinae, vastus lateralis, semitendinosus, rectus femoris, gastrocnemius)	10 healthy	Robotic knee exoskeleton for locomotion mode assistance based on admittance control
Hua et al [74]	DNN	6	standing/transition level walking stair ascent stair descent ramp ascent ramp descent	accuracy	99.7%	Genetic Algorithm Particle Swarm Optimization	absolute autoencoder (for joint angles) IMU (back) GRF connecting rod sensors		Heavy load lifting
Goh et al [43]	SSRL (a) SVM-FS (b) SVM-PCA (c) RF-FS (d)	4	walking without exoskeleton walking with exoskeleton at: Zero-torque Low assistive torque High assistive torque	Accuracy (wide spectral frequencies) (prominent spectral frequencies)	77.8 ± 1.8% (a) 74.3 ± 1.6% (b) 64.3 ± 1.8% (c) 65.9 ± 1.8% (d) 72.9 ± 1.7% (a) 70.2 ± 1.6% (b) 54.8 ± 2.0% (c)	Adam Algorithm	EEG (20 channels)	30 healthy (3 excluded)	-

TABLE 2. *(Continued.)* **Locomotion mode.**

					58.9 ± 1.7% (d)				
Chinimilli et al [81]	fuzzy inference algorithm	3	level walking uphill walking downhill walking	-	-	-	smart shoes IMUs (thigh and shank) EMG (for testing only) Motion capture	3 healthy	Knee assistive device with automatic virtual impedance modulation
Parri et al [90]	Fuzzy logic	3	level walking Stair ascent Stair descent	accuracy	99.4%	-	sensitive insoles (64 optoelectronic sensors) encoders (hip joint angles)	6 healthy	Powered orthosis for hip assistance
Huo et al [83]	Fuzzy logic	5	Level walking Stair ascent Stair descent Slope ascent Slope descent	accuracy latency	97.7% (normal) 97% (abnormal) < 32 ± 8.3% of a step	-	Absolute encoder (hip, knee, and ankle) IMUs	4 healthy	Walking assistance using hybrid power assistive control
Novak et al [91]	DT	2	Intention for gait initiation and termination	Median AE (gait initiation/ IMUs/ within-subject trials) Accuracy (gait termination/ IMUs/ within-subject trials)	~0.08 s (onset) < 0.05 s (toe-off) > 80%	-	IMUs (thigh, shank, upper arm, foot) foot pressure sensors	10 healthy	Assist to initiate or terminate a step based on intention
Zhang et al [92]	MKL	4	Intention for: Stopping Walking Turning left Turning right	accuracy	74.5% (healthy) 68.4% (SCI)	-	EEG (64 channels placed following 10-20 international system)	1 healthy 1 SCI	Restoration of movement for patients with motor disabilities and induction of cortical plasticity
Gui et al [93]	LDA	4	Intention for: Stopping Level walking Acceleration Deceleration	Recognition rate of steady-state (ROS) Duration of transient state (DOT)	92.40% 1.7 seconds	-	EEG	6 healthy	Admittance control exoskeleton for rehabilitation and motor recovery for paraplegics
Lopez-Larraz et al [94]	SDA	1	Intention for gait initiation	accuracy	88.44 ± 14.56% (healthy) 77.61 ± 14.72% (SCI)	-	EEG (32 channels)	3 healthy 4 SCI	Assist-as-needed exoskeleton for rehabilitation and motor recovery of patients with paralysis
Zheng et al [95]	CCA	3	Intention for motion patterns: Standing Level walking Squatting	Accuracy	> 90% (EEG – offline) > 90% (multimodal – online)	-	EEG Sensor for joint position Sensor for foot pressure	4 healthy	-

TABLE 3. Torque and moment.

Authors	Model	Parameter	Performance Metric	Value of Performance Metric	Sensors	Sample	Purpose
Ma et al [73]	KRLS (a) MLPNN (b)	hip joint assist torque	MSE (ranges for five trials)	-32.77 to - 28.05 (a) -13.41 to -11.18 (b)	goniometer (hip and knee joint)	10 healthy	Walking assistance for paraplegics + rehabilitation of stroke patients
Gui et al [96]	RBFNN	active torque of hip and knee	RMSE (experimental session 1-3) correlation coefficient r	2.0 N.m r > 0.8	EMG (quadriceps femoris and bicep femoris) motion states torque sensors (for validation only)	4 healthy	Assist as needed exoskeleton for rehabilitation training for patients with lower-limb paralysis
Xiong et al [97]	NN	internal joint moment	NRMSE	< 7.89%	EMG Joint angles	8 healthy	Exoskeleton for motor rehabilitation
Xiong et al [98]	ELM	Joint moment	VAF	-	EMG (10 muscles)	10 healthy (online database)	Exoskeleton control

3) LEAST SQUARE METHOD

The kernel recursive least square method is implemented by Ma *et al.* [73] for hip assist torque prediction, outperforming the MLPNN. The mean square errors for five trials where between −11.18 and −13.41.

The least square method is implemented Boudali *et al.* [107] for hip and knee joint trajectory prediction. This method resulted in larger RMS errors when compared to the RNN. Furthermore, it was limited to performing static mappings rather than dynamic mappings.

4) PRINCIPAL COMPONENT ANALYSIS AND BEST LINEAR UNBIASED ESTIMATION

Complementary limb motion estimation (CLME) is used in some wearable robotics, particularly for patients with hemiplegia, in which a healthy limb is used to produce a reference trajectory for a pathological limb based on a mapping function. The reference trajectories produced could be angles or trajectories. Vallery *et al.* [108], evaluated the use of CLME which either uses principal component analysis (PCA) or best linear unbiased estimation (BLUE) for the generation of trajectories, comparing it to impedance control (fixed trajectory) and zero-torque control. Their evaluation was based on a few criteria, which included monitoring the amount of power delivered by the exoskeleton in the different control modes, as well as the distortive impact of this method on the muscle activity and the kinematics of gait. Compared to impedance control, using CLME showed to produce more natural walking patterns. PCA-CLME also performed worse than BLUE-CLME.

Probabilistic principal component analysis (PPCA) model is implemented by Tanghe *et al.* [85] for the prediction of gait trajectories. The model is capable of predicting motions over a short time horizon but fails for longer time horizons.

PCA is implemented by Hassan et al [109]. The authors investigated the efficacy of synergy-based control, also referred to as complementary limb motion estimation (CLME). Intended for patients with hemiparesis, the kinematics of the healthy limb and an assistive cane were used to estimate the reference trajectory of the limb with weakness. The reference trajectory was the input to a proportional differential (PD) controller, which controls a single limb HAL exoskeleton. Synergies of the limbs of healthy people were first identified to be able to map the relationship between the healthy and affected limbs of patients with hemiparesis. Synergy-based control was compared to autonomous control.

E. OTHER

The intention to perform dorsiflexion has been decoded using EEG signals by Xu et al [110], for controlling a motorized active foot orthosis. The authors aimed to control the dorsiflexion of a motorized ankle-foot orthosis by having the user imagine dorsiflexion to provide timely stimulation that will promote cortical plasticity for stroke patients. The importance of appropriate stimulation timing correlates with the Hebbian rule that states that 'neurons that fire together, wire together'. Using locality preserving projections (LPP) and a linear discriminant classifier (LDC), movement related cortical potentials (MRCP) were detected. The LPP-MRCP performed a signal versus noise classification and two consecutive 'signal' classifications indicate an MRCP. The classifier was tested on 10 healthy subjects, with a true prediction rate of 73.0 ± 10.3%. To evaluate whether cortical plasticity was induced, transcranial magnetic stimulation (TMS) before, right after and 30 minutes post the 15 min BCI-MAFO was performed. The 87.2% increase of MEP post BCI-MAFO demonstrated cortical plasticity.

V. DISSCUSION AND CONCLUSION

This systematic literature review presented an overview of intelligent algorithms used to obtain parameters of gait for controlling wearable lower limb robotics, such as exoskeletons and orthoses. While unified in their goal of supporting the body in walking and performing various locomotion activities, they varied in their control algorithms, functional purpose and sensors used.

A. GAIT PARAMETER

Several classification and regression models have been implemented for the identification of gait phases, locomotion modes, torque/moments and joint angle trajectories. The type

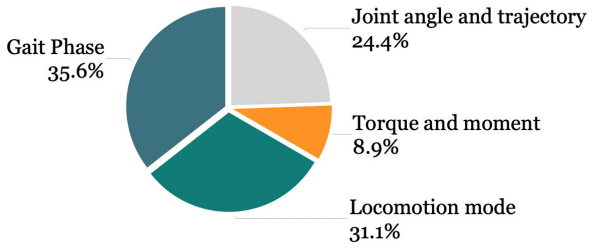

FIGURE 5. Four main gait parameters have been detected or predicted using intelligent algorithms for the control of lower limb robots. The pie chat illustrates the distribution of the gait parameters in the reviewed papers. A large proportion of papers are on gait phases.

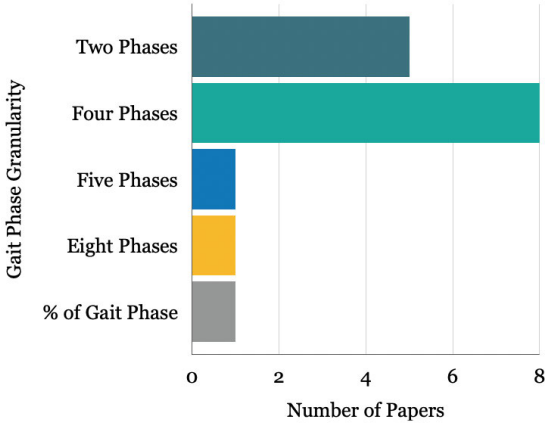

FIGURE 6. Number of phases identified in the reviewed papers.

of parameter that needs to be detected will depend on several factors including (i) the type of control. Gait phases for instance can be used for switching between discrete control modes, while joint trajectory prediction can be used as feedforward to the controller, to enhance stability by compensating for the time delays. Having future information about the trajectories or intent can allow smoother transitions between the control modes [85]. The type of parameter detected is also dependent on (ii) the functional purpose of the exoskeleton. For example, intention derived from muscle activity can be mapped to a discrete number of control modes. This is appropriate for neurorehabilitation applications where the intention information is used as a 'trigger' to initiate timely and appropriate movement of the exoskeleton. Other modes of neurorehabilitation and other functional purposes may require mapping the intention derived from muscle activity to a continuous signal, such as the desired joint torque [47]. The functional purpose and type of control would in turn depend on (iii) the patient's condition and disease. An exoskeleton can be used for locomotion assistance, and/or rehabilitation where it can be used as compensation due to limb amputation or paralysis, or for promoting complete or partial neural recovery caused by neurological injuries, including strokes [47]. These factors should be taken into consideration when choosing the parameter.

The proportion of the parameters in relation to all of the papers reviewed is as follows: 35.6% gait phase, 31.1% locomotion mode, 24.4% joint angle and trajectory and 8.9% torque and moment.

The maximum number of gait phases is eight, yet most of the researchers detected a fewer number in their implementations. Approximately 50% of the papers identified four phases, 30% identified two phases and only one implementation identified all eight phases. Some authors reported that identifying a low number of discrete phases is sufficient for their robotic applications. An alternative to finding a discrete number of gait phases has also been presented, where the percentage of the gait phase was determined instead. This approach obviates the need to have clear features identifying the start and end of each phase.

As for locomotion mode identification, the number of modes detected varied, from as little as one mode, where intention for gait initiation was identified, to detecting fifteen modes which include standing, sitting, walking at different speeds, walking up a slope, and other static and dynamic states. Overall, the most commonly identified locomotion modes are level walking, ascending and descending stairs/ramp, and sitting/standing. The number of modes should be dictated as per the device's design, intended purpose, and users.

Joint angles and trajectories have been identified by several authors. A reference trajectory can be generated and used as input to a controller. Complementary limb motion estimation (CLME) was used, whereby joint trajectories of a healthy limb are utilized to generate trajectories for a pathological limb, such as in the case with patients with hemiparesis. The least commonly detected gait parameter was joint torque/moment, only 8.9% of all the papers reviewed.

A few papers have identified multiple parameters together, mostly gait phases with locomotion modes, while the remaining papers detected one gait parameter only.

B. ALGORITHM

Two main types of algorithms have been used for parameter detection/prediction. Classification models were used to identify a discrete number of gait phases or locomotion modes, and regression models were used to predict continuous kinematic or kinetic trajectories, for estimating joint angles or torques and moments.

Some authors implemented several machine learning models which allowed for comparing their performance while keeping other influential factors such as types of sensors, signal processing, and type and size of input/testing data, constant. A wide range of algorithms was used to detect gait phases, including neural networks, deep neural networks, SVMs, KNN, fuzzy logic etc. Accuracies for gait phase detection ranged from as low as ∼70% up to ∼98%.

Similarly, a wide range of algorithms were used for locomotion mode identification. Most of the implementations that detected three locomotion modes achieved an accuracy greater than 95%. The diversity of algorithms was lower for torque and moment predictions, which were predominantly predicted with neural networks. Similarly, neural networks

TABLE 4. Joint trajectory and angle.

Authors	Model	Parameter	Performance Metric	Value of Performance Metric	Optimization Algorithm	Sensors	Sample	Purpose
Kutilek et al [99]	NN	Joint angles			Backpropagation	Motion capture	10 healthy	Exoskeleton for rehabilitation
Boudali et al [107]	LRNN (a) LS (b)	hip and knee joint trajectories	RMS	1.36º (hip joint) (a) 2.48º (knee joint) (a)	Levenberg-Marquardt back-propagation (a)	Motion capture	9 healthy	Rehabilitation exoskeleton that assists with locomotion tasks (involves the use of cane)
Mazumder et al [101]	RBFNN	joint trajectories	Tracking error	~2º (hip) 8-10º (knee)	-	IMUs (thigh, shank, torso, foot) EMG sensors (vastus medialis, medialis hamstring, vastus laterialis, rectus femoris - for gait phases) Foot pressure sensor (for gait phases)	5 healthy	Exoskeleton with intention-based adaptive trajectory control
Lee et al [102]	RBFNN and MLPNN	Joint angles of healthy and pathological leg	accuracy absolute error rate	97.5% 0.25º	error backpropagation algorithm (for MLPNN)	EMG (recuts femoris) tilt sensor (shin center)		-
Xie et al [103]	GS-GRNN (a) BPNN (b)	joint angles	Prediction time RMSE	2.38s (a) 16.029s (b) 0.7353 hip (a) 2.6998 knee (a) 3.8373 ankle (a)	Golden selection algorithm (a) Levenberg-Marquardt algorithm (b)	EMG (rectus femoris, semitendinosus, biceps femoris) Joint angle sensor plantar pressure sensor	6 healthy	-
Wang et al [104]	Elam NN (a) BPNN (b) GRNN (c) LSSVM (d)	Joint angles	RMSE (low speed without load conditions)	4.0854 (a) 8.9152 (b) 8.7564 (c) 8.6982 (d)	Backpropagation (a)	EMG (biceps femoris gastrocnemius, rectus femoral, vastus medialis, semitendinosus) Codamotion (for evaluation only)	12 healthy	-
Gomes et al [105]	MLPNN	Joint trajectories (position, velocity and acceleration)	-	(Refer to Figure 14 in [105])	-	-	1 healthy	Active orthosis that adapts gait trajectories based on walking speed
Wu et al [106]	AENN	Hip and knee joint trajectories	Individualized gait pattern generation Correlation coefficient (ρ) mean absolute deviation (MAD)	0.99 (right hip) 0.97 (right knee) 0.98 (left hip) 0.98 (left knee) 2.60 (right hip) 3.40 (right knee) 2.62 (left hip)	-	Motion Capture (Noitom^{TM})	33 healthy	Individual trajectory generation for sharing lower limb exoskeleton (SLEX)

TABLE 4. *(Continued.)* **Joint trajectory and angle.**

				3.64 (left knee)				
Vallery et al [108]	PCA-CLME BLUE-CLME	Joint trajectories	-	-	-	Torque & angle trajectories (hip and knee joint) EMG (tibialis anterior, gastrocnemius, bicep femoris, rectus femoris -for evaluation)	9 healthy	
Tanghe et al [85]	PPCA	Hip, knee and ankle joint trajectories	Mean Error	Close to zero (refer to Table III in [85])	-	Vicon cameras split belt treadmill for GRF (for segmentation)	28 healthy without exo + 5 healthy with exo	feedforward to exoskeleton control algorithms, as compensation to control time delays
Hassan et al [109]	PCA	Joint trajectories of the affected limb	-	-	-	IMUs (thigh, shank and cane) Motion capture system (for verification)	5 patients with hemiparesis	

were primarily used for prediction of joint angles and trajectories followed by PCA.

Approximately, only 15% of the papers reviewed implemented deep learning models, mostly for gait phases. When deep learning models such as LSTM-DNN, DM-CNN, SSRL, and LSTM were compared to other shallow machine learning implementations, they were found to outperform in accuracy and F-score metrics. The presented results encourage further studies.

When reporting the performance of the machine learning models, multiple performance metrics have been used including accuracy, root mean square error (RMSE), F-score, precision and recall rates, as well as delay times. While included in some, the duration of computation and the delay of the prediction have not been considered by all the authors. For real-time applications, this is a crucial factor to be considered when choosing a model or a type of sensor, since even high accuracy models cannot be used if the delay time for predictions or computation durations are significantly large, making real-time control of exoskeleton or orthosis not viable.

There have been numerous combinations of sensors to measure data to be used as input for the models. Some included wearable sensors such as IMUs, foot pressure sensors, and EMG electrodes. While others used non-wearable sensors such as Motion Capture Systems, and ground force plates (measure ground reaction force). Although sensors in smartphones have been used in gait analysis [111], they have not been deployed in the papers included in this review. There are advantages and disadvantages of each of the sensors and the signals they measure. IMUs which measure acceleration signals suffer from drift, and they have been remedied by calibrating the value with every step. A method to address this issue has been proposed by Qui *et al.* [112].

There have been single modality approaches where the input of the algorithm is based on data from a single sensor such as an IMU or EMG only and multi-modality approaches where it's a combination of multiple sensors. Optimal location for sensor placement has been frequently studied [113]. There seemed to be preferences for specific sensing modalities based on the parameter predicted. IMU sensors have been commonly used for gait phase detection, whereas EEG has been commonly used for locomotion modes and not for any other parameter. Torque/moment and joint angle trajectory predictions predominantly used EMG.

It's important to make a distinction between sensors that collect measurements to be used as input to algorithms, and between those that collect measurements to segment data collected by another sensor that will be input to machine learning models, or to produce ground truth labels for supervised learning algorithms. One of the most commonly used sensors for segmentation or labelling of gait phases is foot pressure sensors. The same applies to other sensors such as motion capture systems which were also either used as an input or to compare the motion capture measurements to those predicted by machine learning models, as motion capture systems are considered the 'gold standard' for some measurements.

There have been varied choices on whether the accelerometer, gyroscope, or both would be used as well as the number of axes considered. Also, the same measurement can be made using multiple sensors. For example, joint angles could be measured with a goniometer or motion capture system but can also be derived using signals from IMU using quaternion calculations. The choice of sensors will impact performance when comparing wearable and non-wearable sensors. Thus, algorithms trained with data from motion capture systems

may demonstrate lower performance when data from wearable sensors are replaced in the actual implementation.

The type of sensor had an impact on detecting locomotion mode. Implementations involving EEG or EMG sensors had lower prediction accuracies, ranging between 68.4%-92.4%, while implementation utilizing other sensors such as IMUs had accuracies mostly above 90%. For torque and moment prediction, EMG and joint angle sensors were predominantly used.

C. TRAINING DATASET

In the identified studies, the number of participants in the testing of the proposed models is very small (as little as one participant in some cases). This will cause an issue particularly for generalised models that need to capture the inter-subject variability. The highest number reached to around thirty participants. Other papers ranged around ten participants. Studies have shown that algorithms that are trained on a group of participants of people and tested on data from other participants perform worse than personalised models, which learned the gait patterns from a single person and was tested on unseen data from that person. Ideally, achieving higher performance with a generalised model is more desirable, yet if inter-subject variability remains high even among people of the same anthropometrics and gait conditions, leading to lower performance when tested on 'unseen' subjects, individual models may be needed.

The environmental conditions in which the training sets were recorded also have an impact on the real-time performance of the algorithms. Most of the data collected involved experiments in labs, usually under constrained environments. For some studies, walking speeds have been set (due to using treadmills), others involved self-selected speeds. These conditions may perturb natural gait patterns, which usually experience more stochasticity and noise in real environments. Therefore the performance of some of the models presents an ''upper-bound on the performance'' [114], and some deterioration in performance should be expected.

D. FUTURE WORK

Robotic devices have been developing rapidly, so are the models used for controlling them. This paper presents a range of state-of-the-art models that have been currently used, and the different parameters researchers have been investigating. Both classification and regression methods have been successfully integrated with the controllers of exoskeletons, as demonstrated by the papers that applied these algorithms to control their exoskeleton. As previously discussed, the methods chosen are dependent on the type of controller, functional purpose of the exoskeleton, and the disease and condition of the patient. However, further research needs be conducted to compare and contrast the methods. The integration of one or multiple methods with controllers should also be further investigated.

One of the important issues that needs to be addressed is the lack of pathological gait datasets. This is a known limitation across the majority of the papers, whereby models presented need to be trained/tested on pathological gait patterns. In the presence of pathological gait data, transfer learning can be used to increase the model's adaptability to other gait patterns. Knowledge gained in identifying healthy gait parameters can be transferred to pathological gait, particularly if the available datasets for users with pathologies are small [115], [116]. The need for more training data is not limited to including pathological gait. The models need representative data to make accurate predictions. The data sets need to include gait patterns obtained while the users are wearing an exoskeleton, in zero-torque mode, or assistive modes since this alters gait patterns. It should also include users walking at a range of speeds.

Furthermore, the classification models used for detecting gait phases or locomotion modes detect activities only. It may be beneficial to develop algorithms that are capable of assessing the activity [117], since that will enable evaluating the current state of the user of the robotic device and monitor how their gait progresses with its use. This goes along with the need to develop explainable AI, which allows scientist and clinicians to gain insight on how algorithms make their predictions, but also further our understanding of gait analyses. For instance, explainable AI is particularly significant in decoding intention from brain signals, as this will increase our understanding of the brain, and the role of its regions.

Human-robot interaction requires awareness of the state of the user, which all of these algorithms can achieve. However, there is also a need to enhance environmental awareness, such as models that are capable of detecting the type of terrain the user is walking on and adapt the assistance accordingly.

REFERENCES

[1] V. Kumar, Y. V. Hote, and S. Jain, ''Review of exoskeleton: History, design and control,'' in *Proc. 3rd Int. Conf. Recent Develop. Control, Autom. Power Eng. (RDCAPE)*, Oct. 2019, pp. 677–682, doi: 10.1109/RDCAPE47089.2019.8979099.

[2] *Research and Development Prototype for Machine Augmentation of Human Strength and Endurance HARDIMAN I Project*, Gen. Electr. Company Corporate Res. Develop., Schenectady, NY, USA, 1971.

[3] T. Zhang and H. H. Huang, ''A lower-back robotic exoskeleton: Industrial handling augmentation used to provide spinal support,'' *IEEE Robot. Automat. Mag.*, vol. 25, no. 2, pp. 95–106, Jun. 2018, doi: 10.1109/MRA.2018.2815083.

[4] A. S. Khan, D. C. Livingstone, C. L. Hurd, J. Duchcherer, J. E. Misiaszek, M. A. Gorassini, P. J. Manns, and J. F. Yang, ''Retraining walking over ground in a powered exoskeleton after spinal cord injury: A prospective cohort study to examine functional gains and neuroplasticity,'' *J. Neuro-Eng. Rehabil.*, vol. 16, no. 1, p. 145, Nov. 2019, doi: 10.1186/s12984-019-0585-x.

[5] Z. F. Lerner, D. L. Damiano, and T. C. Bulea, ''A lower-extremity exoskeleton improves knee extension in children with crouch gait from cerebral palsy,'' *Sci. Transl. Med.*, vol. 9, no. 404, Aug. 2017, Art. no. eaam9145, doi: 10.1126/scitranslmed.aam9145.

[6] F. Di Russo, M. Berchicci, R. L. Perri, F. R. Ripani, and M. Ripani, ''A passive exoskeleton can push your life up: Application on multiple sclerosis patients,'' *PLoS ONE*, vol. 8, no. 10, Oct. 2013, Art. no. e77348, doi: 10.1371/journal.pone.0077348.

[7] S. Bai, G. S. Virk, and T. G. Sugar, Eds., *Wearable Exoskeleton Systems: Design, Control and Applications*. London, U.K.: The Institution of Engineering and Technology, 2018.

[8] A. B. Zoss, H. Kazerooni, and A. Chu, ''Biomechanical design of the Berkeley lower extremity exoskeleton (BLEEX),'' *IEEE/ASME Trans. Mechatronics*, vol. 11, no. 2, pp. 128–138, Apr. 2006, doi: 10.1109/TMECH.2006.871087.

[9] C. J. Walsh, K. Endo, and H. Herr, "A quasi-passive leg exoskeleton for load-carrying augmentation," *Int. J. Humanoid Robot.*, vol. 4, no. 3, pp. 487–506, 2007, doi: 10.1142/S0219843607001126.
[10] K. Suzuki, G. Mito, H. Kawamoto, Y. Hasegawa, and Y. Sankai, "Intention-based walking support for paraplegia patients with robot Suit HAL," *Adv. Robot.*, vol. 21, no. 12, pp. 1441–1469, 2007, doi: 10.1163/156855307781746061.
[11] S. Wang, L. Wang, C. Meijneke, E. Van Asseldonk, T. Hoellinger, G. Cheron, Y. Ivanenko, V. La Scaleia, F. Sylos-Labini, M. Molinari, and F. Tamburella, "Design and control of the MINDWALKER exoskeleton," *IEEE Trans. Neural Syst. Rehabil. Eng.*, vol. 23, no. 2, pp. 277–286, Mar. 2015, doi: 10.1109/TNSRE.2014.2365697.
[12] H. Herr, "Exoskeletons and orthoses: Classification, design challenges and future directions," *J. NeuroEng. Rehabil.*, vol. 6, no. 1, pp. 1–9, Dec. 2009, doi: 10.1186/1743-0003-6-21.
[13] M. C. Faustini, R. R. Neptune, R. H. Crawford, and S. J. Stanhope, "Manufacture of passive dynamic ankle–foot orthoses using selective laser sintering," *IEEE Trans. Biomed. Eng.*, vol. 55, no. 2, pp. 784–790, Feb. 2008, doi: 10.1109/TBME.2007.912638.
[14] J. A. Blaya and H. Herr, "Adaptive control of a variable-impedance ankle-foot orthosis to assist drop-foot gait," *IEEE Trans. Neural Syst. Rehabil. Eng.*, vol. 12, no. 1, pp. 24–31, Mar. 2004, doi: 10.1109/TNSRE.2003.823266.
[15] B. Chen, H. Ma, L. Y. Qin, F. Gao, K. M. Chan, S. W. Law, L. Qin, and W. H. Liao, "Recent developments and challenges of lower extremity exoskeletons," *J. Orthopaedic Transl.*, vol. 5, pp. 26–37, Apr. 2016, doi: 10.1016/j.jot.2015.09.007.
[16] H. F. N. Al-Shuka and R. Song, "On low-level control strategies of lower extremity exoskeletons with power augmentation," in *Proc. 10th Int. Conf. Adv. Comput. Intell. (ICACI)*, Mar. 2018, pp. 63–68, doi: 10.1109/ICACI.2018.8377581.
[17] H. F. N. Al-Shuka, R. Song, and C. Ding, "On high-level control of power-augmentation lower extremity exoskeletons: Human walking intention," in *Proc. 10th Int. Conf. Adv. Comput. Intell. (ICACI)*, Mar. 2018, pp. 169–174, doi: 10.1109/ICACI.2018.8377601.
[18] J. Vantilt, K. Tanghe, M. Afschrift, A. K. Bruijnes, K. Junius, J. Geeroms, E. Aertbeliën, F. De Groote, D. Lefeber, I. Jonkers, and J. De Schutter, "Model-based control for exoskeletons with series elastic actuators evaluated on sit-to-stand movements," *J. Neuroeng. Rehabil.*, vol. 16, no. 1, p. 65, 2019, doi: 10.1186/s12984-019-0526-8.
[19] H. Zhao, Z. Wang, S. Qiu, Y. Shen, and J. Wang, "IMU-based gait analysis for rehabilitation assessment of patients with gait disorders," in *Proc. 4th Int. Conf. Syst. Informat. (ICSAI)*, Nov. 2017, pp. 622–626, doi: 10.1109/ICSAI.2017.8248364.
[20] W. Zeng, C. Yuan, Q. Wang, F. Liu, and Y. Wang, "Classification of gait patterns between patients with Parkinson's disease and healthy controls using phase space reconstruction (PSR), empirical mode decomposition (EMD) and neural networks," *Neural Netw.*, vol. 111, pp. 64–76, Mar. 2019, doi: 10.1016/j.neunet.2018.12.012.
[21] M. Hadizadeh, S. Amri, H. Mohafez, S. A. Roohi, and A. H. Mokhtar, "Gait analysis of national athletes after anterior cruciate ligament reconstruction following three stages of rehabilitation program: Symmetrical perspective," *Gait Posture*, vol. 48, pp. 152–158, Jul. 2016, doi: 10.1016/j.gaitpost.2016.05.002.
[22] Y. Wahab and N. A. Bakar, "Gait analysis measurement for sport application based on ultrasonic system," in *Proc. IEEE 15th Int. Symp. Consum. Electron. (ISCE)*, Jun. 2011, pp. 20–24, doi: 10.1109/ISCE.2011.5973775.
[23] O. Dehzangi, M. Taherisadr, and R. ChangalVala, "IMU-based gait recognition using convolutional neural networks and multi-sensor fusion," *Sensors*, vol. 17, no. 12, p. 2735, 2017, doi: 10.3390/s17122735.
[24] S. Tao, X. Zhang, H. Cai, Z. Lv, C. Hu, and H. Xie, "Gait based biometric personal authentication by using MEMS inertial sensors," *J. Ambient Intell. Humanized Comput.*, vol. 9, no. 5, pp. 1705–1712, Oct. 2018, doi: 10.1007/s12652-018-0880-6.
[25] F. Sun, W. Zang, R. Gravina, G. Fortino, and Y. Li, "Gait-based identification for elderly users in wearable healthcare systems," *Inf. Fusion*, vol. 53, pp. 134–144, Jan. 2020, doi: 10.1016/j.inffus.2019.06.023.
[26] N. Shibuya, B. T. Nukala, A. I. Rodriguez, J. Tsay, T. Q. Nguyen, S. Zupancic, and D. Y. C. Lie, "A real-time fall detection system using a wearable gait analysis sensor and a support vector machine (SVM) classifier," in *Proc. 8th Int. Conf. Mobile Comput. Ubiquitous Netw. (ICMU)*, Jan. 2015, pp. 66–67, doi: 10.1109/ICMU.2015.7061032.
[27] I. Birch, T. Birch, and D. Bray, "The identification of emotions from gait," *Sci. Jus.*, vol. 56, no. 5, pp. 351–356, 2016, doi: 10.1016/j.scijus.2016.05.006.
[28] C. Prakash, R. Kumar, and N. Mittal, "Recent developments in human gait research: Parameters, approaches, applications, machine learning techniques, datasets and challenges," *Artif. Intell. Rev.*, vol. 49, no. 1, pp. 1–40, Jan. 2018, doi: 10.1007/s10462-016-9514-6.
[29] A. S. Alharthi, S. U. Yunas, and K. B. Ozanyan, "Deep learning for monitoring of human gait: A review," *IEEE Sensors J.*, vol. 19, no. 21, pp. 9575–9591, Nov. 2019, doi: 10.1109/JSEN.2019.2928777.
[30] A. Behboodi, N. Zahradka, H. Wright, J. Alesi, and S. C. K. Lee, "Real-time detection of seven phases of gait in children with cerebral palsy using two gyroscopes," *Sensors*, vol. 19, no. 11, p. 2517, Jun. 2019, doi: 10.3390/s19112517.
[31] W. Hassani, S. Mohammed, H. Rifai, and Y. Amirat, "EMG based approach for wearer-centered control of a Knee joint actuated orthosis," in *Proc. IEEE/RSJ Int. Conf. Intell. Robots Syst.*, Nov. 2013, pp. 990–995, doi: 10.1109/IROS.2013.6696471.
[32] J. Taborri, E. Palermo, S. Rossi, and P. Cappa, "Gait partitioning methods: A systematic review," *Sensors*, vol. 16, no. 1, pp. 40–42, 2016, doi: 10.3390/s16010066.
[33] S. Chen, J. Lach, B. Lo, and G.-Z. Yang, "Toward pervasive gait analysis with wearable sensors: A systematic review," *IEEE J. Biomed. Health Inform.*, vol. 20, no. 6, pp. 1521–1537, Nov. 2016, doi: 10.1109/JBHI.2016.2608720.
[34] R. Caldas, T. Fadel, F. Buarque, and B. Markert, "Adaptive predictive systems applied to gait analysis: A systematic review," *Gait Posture*, vol. 77, pp. 75–82, Mar. 2020, doi: 10.1016/j.gaitpost.2020.01.021.
[35] R. Caldas, M. Mundt, W. Potthast, F. B. de Lima Neto, and B. Markert, "A systematic review of gait analysis methods based on inertial sensors and adaptive algorithms," *Gait Posture*, vol. 57, pp. 204–210, Sep. 2017, doi: 10.1016/j.gaitpost.2017.06.019.
[36] G. Bao, L. Pan, H. Fang, X. Wu, H. Yu, S. Cai, B. Yu, and Y. Wan, "Academic review and perspectives on robotic exoskeletons," *IEEE Trans. Neural Syst. Rehabil. Eng.*, vol. 27, no. 11, pp. 2294–2304, Nov. 2019, doi: 10.1109/TNSRE.2019.2944655.
[37] E. Alpaydin, "Introduction," in *Introduction to Machine Learning*. Cambridge, MA, USA: MIT Press, 2014, pp. 1–20.
[38] Ł. Kidziński, S. Delp, and M. Schwartz, "Automatic real-time gait event detection in children using deep neural networks," *PLoS ONE*, vol. 14, no. 1, Jan. 2019, Art. no. e0211466, doi: 10.1371/journal.pone.0211466.
[39] J.-Y. Jung, W. Heo, H. Yang, and H. Park, "A neural network-based gait phase classification method using sensors equipped on lower limb exoskeleton robots," *Sensors*, vol. 15, no. 11, pp. 27738–27759, 2015, doi: 10.3390/s151127738.
[40] M. D. S. Sánchez Manchola, M. J. P. Pinto Bernal, M. Munera, and C. A. Cifuentes, "Gait phase detection for lower-limb exoskeletons using foot motion data from a single inertial measurement unit in hemiparetic individuals," *Sensors*, vol. 19, no. 13, p. 2988, Jul. 2019, doi: 10.3390/s19132988.
[41] I. Kang, P. Kunapuli, and A. J. Young, "Real-time neural network-based gait phase estimation using a robotic hip exoskeleton," *IEEE Trans. Med. Robot. Bionics*, vol. 2, no. 1, pp. 28–37, Feb. 2020, doi: 10.1109/tmrb.2019.2961749.
[42] A. Hashemi, Y. Lin, W. McNally, B. Laschowski, B. Hosking, A. Wong, and J. McPhee, "Integration of machine learning with dynamics and control: From autonomous cars to biomechatronics," *CSME Bull.*, pp. 7–8, 2019.
[43] S. K. Goh, H. A. Abbass, K. C. Tan, A. Al-Mamun, N. Thakor, A. Bezerianos, and J. Li, "Spatio–spectral representation learning for electroencephalographic gait-pattern classification," *IEEE Trans. Neural Syst. Rehabil. Eng.*, vol. 26, no. 9, pp. 1858–1867, Sep. 2018, doi: 10.1109/TNSRE.2018.2864119.
[44] M. W. Whittle, *Gait Analysis?: An Introduction*. Amsterdam, The Netherlands: Elsevier, 1991.
[45] D. Levine, J. Richards, and M. W. Whittle, *Whittle's Gait Analysis*, 5th ed. Edinburgh, Scotland: Elsevier, 2012.
[46] N. Özkaya, D. Goldsheyder, M. Nordin, and D. Leger, *Fundamentals of Biomechanics: Equilibrium, Motion, and Deformation*, 4th ed. Cham, Switzerland: Springer, 2017.
[47] D. P. Losey, C. G. McDonald, E. Battaglia, and M. K. O'Malley, "A review of intent detection, arbitration, and communication aspects of shared control for physical human–robot interaction," *Appl. Mech. Rev.*, vol. 70, no. 1, pp. 1–19, Jan. 2018, doi: 10.1115/1.4039145.

[48] S. M. Shafiul Hasan, M. R. Siddiquee, R. Atri, R. Ramon, J. S. Marquez, and O. Bai, "Prediction of gait intention from pre-movement EEG signals: A feasibility study," *J. NeuroEng. Rehabil.*, vol. 17, no. 1, pp. 1–16, Dec. 2020, doi: 10.1186/s12984-020-00675-5.

[49] D. Liu, W. Chen, R. Chavarriaga, Z. Pei, and J. D. R. Millán, "Decoding of self-paced lower-limb movement intention: A case study on the influence factors," *Frontiers Human Neurosci.*, vol. 11, pp. 1–12, Nov. 2017, doi: 10.3389/fnhum.2017.00560.

[50] H. Shibasaki and M. Hallett, "What is the bereitschaftspotential?" *Clin. Neurophysiol.*, vol. 117, no. 11, pp. 2341–2356, 2006, doi: 10.1016/j.clinph.2006.04.025.

[51] B. Gudiño-Mendoza, G. Sanchez-Ante, and J. M. Antelis, "Detecting the intention to move upper limbs from electroencephalographic brain signals," *Comput. Math. Methods Med.*, vol. 2016, pp. 1–11, Apr. 2016.

[52] Y. He, D. Eguren, J. M. Azorín, R. G. Grossman, T. P. Luu, and J. L. Contreras-Vidal, "Brain–machine interfaces for controlling lower-limb powered robotic systems," *J. Neural Eng.*, vol. 15, no. 2, Apr. 2018, Art. no. 021004, doi: 10.1088/1741-2552/aaa8c0.

[53] L. Lacourpaille, F. Hug, and A. Nordez, "Influence of passive muscle tension on electromechanical delay in humans," *PLoS ONE*, vol. 8, no. 1, Jan. 2013, Art. no. e53159, doi: 10.1371/journal.pone.0053159.

[54] C. Sammut and G. I. Webb, Eds., "Supervised learning," in *Encyclopedia of Machine Learning*. Boston, MA, USA: Springer, 2010, p. 941.

[55] C. Sammut and G. I. Webb, Eds., "Unsupervised learning," in *Encyclopedia of Machine Learning*. Boston, MA, USA: Springer, 2010, p. 1009.

[56] P. Stone, "Reinforcement learning," in *Encyclopedia of Machine Learning*, C. Sammut G. I. Webb, Eds. Boston, MA, USA: Springer, 2010, pp. 849–851.

[57] B. E. Boser, I. M. Guyon, and V. N. Vapnik, "A training algorithm for optimal margin classifiers," in *Proc. 5th Annu. Workshop Comput. Learn. Theory (COLT)*, Pittsburgh, PA, USA. New York, NY, USA: Association for Computing Machinery, 1992, pp. 144–152.

[58] C. Cortes and V. Vapnik, "Support-vector networks," *Mach. Learn.*, vol. 20, no. 3, pp. 273–297, 1995.

[59] N. Cristianini and E. Ricci, "Support vector machines," in *Encyclopedia Algorithms*, M.-Y. Kao, Ed. Boston, MA, USA: Springer, 2008, pp. 928–932.

[60] W. Ertel, *Introduction to Artificial Intelligence*. London, U.K.: Springer, 2011.

[61] J. Fürnkranz, "Decision tree," in *Encyclopedia of Machine Learning*, C. Sammut G. I. Webb, Eds. Boston, MA, USA: Springer, 2010, pp. 263–267.

[62] J. R. Quinlan, "Induction of decision trees," *Mach. Learn.*, vol. 1, no. 1, pp. 81–106, 1986, doi: 10.1007/bf00116251.

[63] S. L. Salzberg, "C4.5: Programs for machine learning," *Mach. Learn.*, vol. 16, no. 3, pp. 235–240, Sep. 1994.

[64] C. Buckner and J. Garson, *Connectionism, Fall 2019. Metaphysics Research Lab*. Stanford, CA, USA: Stanford Univ., 2019.

[65] W. S. McCulloch and W. Pitts, "A logical calculus of the ideas immanent in nervous activity," *Bull. Math. Biophys.*, vol. 5, no. 4, pp. 115–133, 1943.

[66] F. Rosenblatt, "The perceptron: A probabilistic model for information storage and organization in the brain," *Psychol. Rev.*, vol. 65, no. 6, pp. 386–408, 1958, doi: 10.1037/h0042519.

[67] R. Miikkulainen, "Topology of a neural network," in *Encyclopedia of Machine Learning*, C. Sammut G. I. Webb, Eds. Boston, MA, USA: Springer, 2010, pp. 988–989.

[68] S. I. Gallant, *Neural Network Learning and Expert Systems*. Cambridge, MA, USA: MIT Press, 1993.

[69] S. Mirjalili, "Evolutionary radial basis function networks," in *Evolutionary Algorithms and Neural Networks: Theory and Applications*. Cham, Switzerland: Springer, 2019, pp. 105–139.

[70] P. Munro, "Backpropagation," in *Encyclopedia of Machine Learning*, C. Sammut and G. I. Webb, Eds. Boston, MA, USA: Springer, 2010, p. 73.

[71] I. Goodfellow, Y. Bengio, and A. Courville, *Deep Learning*. Cambridge, MA, USA: MIT Press, 2016.

[72] Y. LeCun, P. Haffner, L. Bottou, and Y. Bengio, "Object recognition with gradient-based learning," in *Shape, Contour and Grouping in Computer Vision*. Berlin, Germany: Springer, 1999, pp. 319–345.

[73] Y. Ma, X. Wu, C. Wang, Z. Yi, and G. Liang, "Gait phase classification and assist torque prediction for a lower limb exoskeleton system using kernel recursive least-squares method," *Sensors*, vol. 19, no. 24, p. 5449, Dec. 2019, doi: 10.3390/s19245449.

[74] Y. Hua, J. Fan, G. Liu, X. Zhang, M. Lai, M. Li, T. Zheng, G. Zhang, J. Zhao, and Y. Zhu, "A novel weight-bearing lower limb exoskeleton based on motion intention prediction and locomotion state identification," *IEEE Access*, vol. 7, pp. 37620–37638, 2019, doi: 10.1109/ACCESS.2019.2904709.

[75] N. Nazmi, M. A. A. Rahman, S.-I. Yamamoto, and S. A. Ahmad, "Walking gait event detection based on electromyography signals using artificial neural network," *Biomed. Signal Process. Control*, vol. 47, pp. 334–343, Jan. 2019, doi: 10.1016/j.bspc.2018.08.030.

[76] X. Zhang, S. Sun, C. Li, and Z. Tang, "Impact of load variation on the accuracy of gait recognition from surface EMG signals," *Appl. Sci.*, vol. 8, no. 9, p. 1462, Aug. 2018, doi: 10.3390/app8091462.

[77] T. Zhen, L. Yan, and P. Yuan, "Walking gait phase detection based on acceleration signals using LSTM-DNN algorithm," *Algorithms*, vol. 12, no. 12, p. 253, Nov. 2019, doi: 10.3390/A12120253.

[78] F. Wang, L. Yan, and J. Xiao, "Recognition of the gait phase based on new deep learning algorithm using multisensor information fusion," *Sensors Mater.*, vol. 31, no. 10, pp. 3041–3054, 2019, doi: 10.18494/SAM.2019.2493.

[79] J. D. Farah, N. Baddour, and E. D. Lemaire, "Design, development, and evaluation of a local sensor-based gait phase recognition system using a logistic model decision tree for orthosis-control," *J. NeuroEng. Rehabil.*, vol. 16, no. 1, pp. 1–11, Feb. 2019, doi: 10.1186/s12984-019-0486-z.

[80] S. Pasinetti, A. Fornaser, M. Lancini, M. De Cecco, and G. Sansoni, "Assisted gait phase estimation through an embedded depth camera using modified random forest algorithm classification," *IEEE Sensors J.*, vol. 20, no. 6, pp. 3343–3355, Mar. 2020, doi: 10.1109/JSEN.2019.2957667.

[81] P. T. Chinimilli, Z. Qiao, S. M. R. Sorkhabadi, V. Jhawar, I. H. Fong, and W. Zhang, "Automatic virtual impedance adaptation of a knee exoskeleton for personalized walking assistance," *Robot. Auto. Syst.*, vol. 114, pp. 66–76, Apr. 2019, doi: 10.1016/j.robot.2019.01.013.

[82] C.-F. Chen, Z.-J. Du, L. He, Y.-J. Shi, J.-Q. Wang, G.-Q. Xu, Y. Zhang, D.-M. Wu, and W. Dong, "Development and hybrid control of an electrically actuated lower limb exoskeleton for motion assistance," *IEEE Access*, vol. 7, pp. 169107–169122, 2019, doi: 10.1109/ACCESS.2019.2953302.

[83] W. Huo, S. Mohammed, Y. Amirat, and K. Kong, "Fast gait mode detection and assistive torque control of an exoskeletal robotic orthosis for walking assistance," *IEEE Trans. Robot.*, vol. 34, no. 4, pp. 1035–1052, Aug. 2018, doi: 10.1109/TRO.2018.2830367.

[84] C. Chen, X. Wu, D.-X. Liu, W. Feng, and C. Wang, "Design and voluntary motion intention estimation of a novel wearable full-body flexible exoskeleton robot," *Mobile Inf. Syst.*, vol. 2017, pp. 1–11, Jun. 2017, doi: 10.1155/2017/8682168.

[85] K. Tanghe, F. De Groote, D. Lefeber, J. De Schutter, and E. Aertbelien, "Gait trajectory and event prediction from state estimation for exoskeletons during gait," *IEEE Trans. Neural Syst. Rehabil. Eng.*, vol. 28, no. 1, pp. 211–220, Jan. 2020, doi: 10.1109/TNSRE.2019.2950309.

[86] J. Song, A. Zhu, Y. Tu, Y. Wang, M. A. Arif, H. Shen, Z. Shen, X. Zhang, and G. Cao, "Human body mixed motion pattern recognition method based on multi-source feature parameter fusion," *Sensors*, vol. 20, no. 2, p. 537, Jan. 2020, doi: 10.3390/s20020537.

[87] M. Islam and E. T. Hsiao-Wecksler, "Detection of gait modes using an artificial neural network during walking with a powered ankle-foot orthosis," *J. Biophys.*, vol. 2016, pp. 1–9, Dec. 2016, doi: 10.1155/2016/7984157.

[88] F. Wang, L. Yan, and J. Xiao, "Human gait recognition system based on support vector machine algorithm and using wearable sensors," *Sensors Mater.*, vol. 31, no. 4, pp. 1335–1349, 2019, doi: 10.18494/SAM.2019.2288.

[89] A. C. Villa-Parra, D. Delisle-Rodriguez, T. Botelho, J. J. V. Mayor, A. L. Delis, R. Carelli, A. Frizera Neto, and T. F. Bastos, "Control of a robotic knee exoskeleton for assistance and rehabilitation based on motion intention from sEMG," *Res. Biomed. Eng.*, vol. 34, no. 3, pp. 198–210, Jul. 2018, doi: 10.1590/2446-4740.07417.

[90] A. Parri, K. Yuan, D. Marconi, T. Yan, S. Crea, M. Munih, R. M. Lova, N. Vitiello, and Q. Wang, "Real-time hybrid locomotion mode recognition for lower limb wearable robots," *IEEE/ASME Trans. Mechatronics*, vol. 22, no. 6, pp. 2480–2491, Dec. 2017, doi: 10.1109/TMECH.2017.2755048.

[91] D. Novak, P. Reberšek, S. M. M. De Rossi, M. Donati, J. Podobnik, T. Beravs, T. Lenzi, N. Vitiello, M. C. Carrozza, and M. Munih, "Automated detection of gait initiation and termination using wearable sensors," *Med. Eng. Phys.*, vol. 35, no. 12, pp. 1713–1720, 2013, doi: 10.1016/j.medengphy.2013.07.003.

[92] Y. Zhang, S. Prasad, A. Kilicarslan, and J. L. Contreras-Vidal, "Multiple kernel based region importance learning for neural classification of gait states from EEG signals," *Frontiers Neurosci.*, vol. 11, p. 170, Apr. 2017, doi: 10.3389/fnins.2017.00170.

[93] K. Gui, H. Liu, and D. Zhang, "Toward multimodal human–robot interaction to enhance active participation of users in gait rehabilitation," *IEEE Trans. Neural Syst. Rehabil. Eng.*, vol. 25, no. 11, pp. 2054–2066, Nov. 2017, doi: 10.1109/TNSRE.2017.2703586.

[94] E. López-Larraz, F. Trincado-Alonso, V. Rajasekaran, S. Pérez-Nombela, A. J. del-Ama, J. Aranda, J. Minguez, A. Gil-Agudo, and L. Montesano, "Control of an ambulatory exoskeleton with a brain–machine interface for spinal cord injury gait rehabilitation," *Frontiers Neurosci.*, vol. 10, p. 359, Aug. 2016, doi: 10.3389/fnins.2016.00359.

[95] Y. Zheng, Q. Song, J. Liu, Q. Song, and Q. Yue, "Research on motion pattern recognition of exoskeleton robot based on multimodal machine learning model," *Neural Comput. Appl.*, vol. 32, no. 7, pp. 1869–1877, Apr. 2020, doi: 10.1007/s00521-019-04567-1.

[96] K. Gui, H. Liu, and D. Zhang, "A practical and adaptive method to achieve EMG-based torque estimation for a robotic exoskeleton," *IEEE/ASME Trans. Mechatronics*, vol. 24, no. 2, pp. 483–494, Apr. 2019, doi: 10.1109/TMECH.2019.2893055.

[97] B. Xiong, N. Zeng, H. Li, Y. Yang, Y. Li, M. Huang, W. Shi, M. Du, and Y. Zhang, "Intelligent prediction of human lower extremity joint moment: An artificial neural network approach," *IEEE Access*, vol. 7, pp. 29973–29980, 2019, doi: 10.1109/ACCESS.2019.2900591.

[98] B. Xiong, N. Zeng, Y. Li, M. Du, M. Huang, W. Shi, G. Mao, and Y. Yang, "Determining the online measurable input variables in human joint moment intelligent prediction based on the Hill muscle model," *Sensors*, vol. 20, no. 4, p. 1185, Feb. 2020, doi: 10.3390/s20041185.

[99] P. Kutilek and B. Farkasova, "Prediction of lower extremities' movement by angle-angle diagrams and neural networks," *Acta Bioeng. Biomech.*, vol. 13, no. 2, pp. 57–65, 2011.

[100] P. Kutilek and S. Viteckova, "Prediction of lower extremity movement by cyclograms," *Acta Polytechnica*, vol. 52, no. 1, p. 51, Jan. 2012.

[101] O. Mazumder, A. S. Kundu, P. K. Lenka, and S. Bhaumik, "Multi-channel fusion based adaptive gait trajectory generation using wearable sensors," *J. Intell. Robotic Syst.*, vol. 86, nos. 3–4, pp. 335–351, Jun. 2017, doi: 10.1007/s10846-016-0436-y.

[102] J.-W. Lee and G.-K. Lee, "Gait angle prediction for lower limb orthotics and prostheses using an EMG signal and neural networks," *Int. J. Control. Autom. Syst.*, vol. 3, no. 2, pp. 152–158, 2005.

[103] H. Xie, G. Li, X. Zhao, and F. Li, "Prediction of limb joint angles based on multi-source signals by GS-GRNN for exoskeleton wearer," *Sensors*, vol. 20, no. 4, p. 1104, Feb. 2020, doi: 10.3390/s20041104.

[104] J. Wang, L. Wang, S. M. Miran, X. Xi, and A. Xue, "Surface electromyography based estimation of knee joint angle by using correlation dimension of wavelet coefficient," *IEEE Access*, vol. 7, pp. 60522–60531, 2019, doi: 10.1109/ACCESS.2019.2913959.

[105] M. A. Gomes, G. L. M. Silveira, and A. A. G. Siqueira, "Gait pattern adaptation for an active lower-limb orthosis based on neural networks," *Adv. Robot.*, vol. 25, no. 15, pp. 1903–1925, Jan. 2011, doi: 10.1163/016918611X588899.

[106] X. Wu, D. X. Liu, M. Liu, C. Chen, and H. Gao, "Individualized gait pattern generation for sharing lower limb exoskeleton robot," *IEEE Trans. Autom. Sci. Eng.*, vol. 15, no. 4, pp. 1459–1470, Oct. 2018, doi: 10.1109/TASE.2018.2841358.

[107] A. M. Boudali, P. J. Sinclair, and I. R. Manchester, "Predicting transitioning walking gaits: Hip and knee joint trajectories from the motion of walking canes," *IEEE Trans. Neural Syst. Rehabil. Eng.*, vol. 27, no. 9, pp. 1791–1800, Sep. 2019, doi: 10.1109/TNSRE.2019.2933896.

[108] H. Vallery, E. H. F. van Asseldonk, M. Buss, and H. van der Kooij, "Reference trajectory generation for rehabilitation robots: Complementary limb motion estimation," *IEEE Trans. Neural Syst. Rehabil. Eng.*, vol. 17, no. 1, pp. 23–30, Feb. 2009, doi: 10.1109/TNSRE.2008.2008278.

[109] M. Hassan, H. Kadone, T. Ueno, Y. Hada, Y. Sankai, and K. Suzuki, "Feasibility of synergy-based exoskeleton robot control in hemiplegia," *IEEE Trans. Neural Syst. Rehabil. Eng.*, vol. 26, no. 6, pp. 1233–1242, Jun. 2018, doi: 10.1109/TNSRE.2018.2832657.

[110] R. Xu, N. Jiang, N. Mrachacz-Kersting, C. Lin, G. A. Prieto, J. C. Moreno, J. L. Pons, K. Dremstrup, and D. Farina, "A closed-loop brain–computer interface triggering an active ankle–foot orthosis for inducing cortical neural plasticity," *IEEE Trans. Biomed. Eng.*, vol. 61, no. 7, pp. 2092–2101, Jul. 2014, doi: 10.1109/TBME.2014.2313867.

[111] P. Silsupadol, K. Teja, and V. Lugade, "Reliability and validity of a smartphone-based assessment of gait parameters across walking speed and smartphone locations: Body, bag, belt, hand, and pocket," *Gait Posture*, vol. 58, pp. 516–522, Oct. 2017, doi: 10.1016/j.gaitpost.2017.09.030.

[112] S. Qiu, Z. Wang, H. Zhao, and H. Hu, "Using distributed wearable sensors to measure and evaluate human lower limb motions," *IEEE Trans. Instrum. Meas.*, vol. 65, no. 4, pp. 939–950, Apr. 2016, doi: 10.1109/TIM.2015.2504078.

[113] A. R. Anwary, H. Yu, and M. Vassallo, "Optimal foot location for placing wearable IMU sensors and automatic feature extraction for gait analysis," *IEEE Sensors J.*, vol. 18, no. 6, pp. 2555–2567, Mar. 2018, doi: 10.1109/JSEN.2017.2786587.

[114] P. Slade, R. Troutman, M. J. Kochenderfer, S. H. Collins, and S. L. Delp, "Rapid energy expenditure estimation for ankle assisted and inclined loaded walking," *J. NeuroEng. Rehabil.*, vol. 16, no. 1, pp. 1–10, Jun. 2019, doi: 10.1186/s12984-019-0535-7.

[115] Y. Gao and Y. Cui, "Deep transfer learning for reducing health care disparities arising from biomedical data inequality," *Nature Commun.*, vol. 11, no. 1, pp. 1–8, Dec. 2020, doi: 10.1038/s41467-020-18918-3.

[116] F. Zhuang, Z. Qi, K. Duan, D. Xi, Y. Zhu, H. Zhu, H. Xiong, and Q. He, "A comprehensive survey on transfer learning," *Proc. IEEE*, vol. 109, no. 1, pp. 43–76, Jan. 2021, doi: 10.1109/JPROC.2020.3004555.

[117] M. Seiffert, F. Holstein, R. Schlosser, and J. Schiller, "Next generation cooperative wearables: Generalized activity assessment computed fully distributed within a wireless body area network," *IEEE Access*, vol. 5, pp. 16793–16807, 2017, doi: 10.1109/ACCESS.2017.2749005.

RANIA KOLAGHASSI received the B.Eng. degree in biomedical engineering from the University of Kent, Canterbury, U.K., in 2019, where she is currently pursuing the Ph.D. degree. She is a member of the Intelligent Interactions Research Group and the Kent Assistive Robotics Laboratory (KAROL), School of Engineering, University of Kent. Her research interests include gait analysis, exoskeletons, human–robot interaction, and machine and deep learning for medical and rehabilitative applications.

MOHAMAD KENAN AL-HARES received the B.Eng. degree in computer and communication engineering from Arab International University, Daraa, Syria, the M.Sc. degree in network computing from Coventry University, Coventry, U.K., and the Ph.D. degree in electronic engineering from the University of Kent, Canterbury, U.K. He is currently with the Intelligent Interactions Research Group. He is a member of the Kent Assistive Robotics Laboratory (KAROL), School of Engineering, University of Kent. His research interests include cloud-radio access networks, ethernet fronthaul development for the future mobile networks, and machine and deep learning.

KONSTANTINOS SIRLANTZIS is currently an Associate Professor of intelligent systems with the School of Engineering, University of Kent. He is the Head of the Intelligent Interaction Research Group, Kent, and the Founding Director of the Kent Assistive Robotics Laboratory (KAROL). He has a strong track record in artificial intelligence and neural networks for image analysis and understanding, robotic systems with emphasis in assistive technologies, and pattern recognition for biometrics-based security applications. He has organized and chaired a range of international conferences and workshops, and he has authored over 130 peer-reviewed articles in journals and conferences.